minerals

MDPI

Review

Coal and Coal By-Products as Unconventional Lithium Sources: A Review of Occurrence Modes and Hydrometallurgical Strategies for Metal Recovery

Ewa Rudnik

Faculty of Non-Ferrous Metals, AGH University of Krakow, Al. Mickiewicza 30, 30-059 Krakow, Poland; erudnik@agh.edu.pl

Abstract: Lithium, a critical material for the global development of green energy sources, is anomalously enriched in some coal deposits and coal by-products to levels that may be considered economically viable. Recovering lithium from coal, particularly from coal gangue or coal ashes, offers a promising alternative for extracting this element. This process could potentially lead to economic gains and positive environmental impacts by more efficiently utilizing coal-based waste materials. This review focuses on lithium concentrations in coal and coal by-products, modes of lithium occurrence, methods used to identify lithium-enriched phases, and currently available hydrometallurgical recovery methods, correlated with pretreatment procedures that enable lithium release from inert aluminosilicate minerals. Leaching of raw coal appears inefficient, whereas coal gangue and fly ash are more feasible due to their simpler composition and higher lithium contents. Lithium extraction can achieve recovery rates of over 90%, but low lithium concentrations and high impurity levels in the leachates require advanced selective separation techniques. Bottom ash has not yet been evaluated for lithium recovery, despite its higher lithium content compared to feed coal.

Keywords: coal; coal gangue; coal fly ash; coal bottom ash; extraction; leaching; recycling; speciation; separation

check for updates

Citation: Rudnik, E. Coal and Coal By-Products as Unconventional Lithium Sources: A Review of Occurrence Modes and Hydrometallurgical Strategies for Metal Recovery. *Minerals* **2024**, *14*, 849. https://doi.org/10.3390/min14080849

Academic Editors: Bogale Tadesse, Jonas Addai-Mensah, Girma Woldetinsae and Lisha Dong

Received: 29 July 2024
Revised: 20 August 2024
Accepted: 21 August 2024
Published: 22 August 2024

Copyright: © 2024 by the author. Licensee MDPI, Basel, Switzerland. This article is an open access article distributed under the terms and conditions of the Creative Commons Attribution (CC BY) license (https://creativecommons.org/licenses/by/4.0/).

1. Introduction

Lithium, often called 'white gold' or 'white petroleum', is a silvery-white and highly valued element, classified as one of 34 critical materials for the European Union [1], the United States [2], and other countries [3], and is a key component in the effort to abandon fossil fuels and transition to clean energy [4,5]. Worldwide demand for lithium has continued to increase rapidly in recent years, driven primarily by its prominent application in rechargeable batteries for electric vehicles, portable electrical equipment, mobile electronics, stationary energy storage, etc. [6–8]. In 2023, battery applications alone accounted for 87% of total lithium consumption (Figure 1a) [9]. This trend is underscored by the intensification in lithium mine production over the last decade, reaching a record value of 180,000 metric tons in 2023, compared to an average annual level of about 32,400 metric tons in the period from 2010 to 2015 [9].

The world leaders in lithium production are currently Australia, Chile, and China, which together supply approximately 90% of the element, mainly carbonate, hydroxide, and oxide [9]. In Australia, lithium is derived from spodumene, the primary lithium-bearing mineral [10,11]. Chile extracts lithium chloride from lithium-rich brines pumped from beneath the Earth's surface into evaporation ponds in Chile's Atacama Desert [12]. Remarkably, Salar Atacama has the highest known concentration of lithium, at about 1500 ppm. China's lithium sources include brines, mainly of sulfate and carbonate types [13], as well as spodumene and lepidolite minerals [14,15].

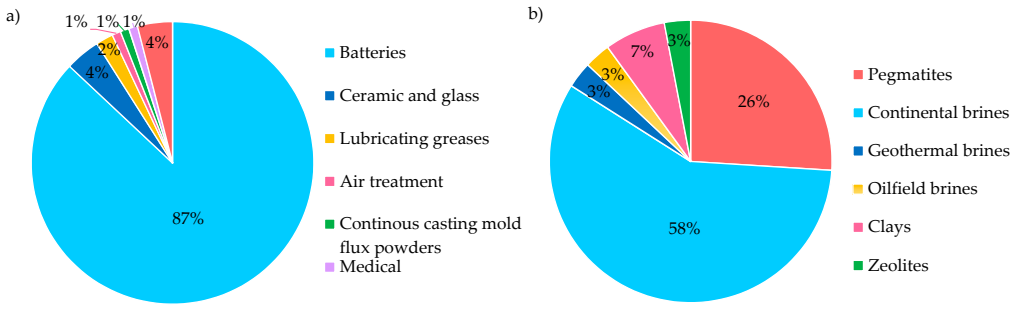


Figure 1. Main global end uses (**a**) and resources (**b**) of lithium (based on [9,10]).

Although hard rocks (pegmatites) and liquid salar brines (salt lakes) represent the primary commercial natural sources of lithium (Figure 1b) [16–19], other types of deposits are regarded as significant due to their large volumes of lithium-bearing minerals (Table 1). These include some hard rock minerals (e.g., zinnwaldite, petalite, amblygonite, and eucryptite) and sedimentary ores consisting of clay, silicate, or aluminum minerals (e.g., jadarite, hectorite) [11,14–19].

Table 1. Lithium concentration ranges in natural and secondary sources [16,17,20–32].

Lithium Source	Li Concentration, wt% (or ppm)
Ores	
Spodumene $Li_2O{\cdot}Al_2O_3{\cdot}4SiO_2$	1.9–3.3
Lepidolite $LiF{\cdot}KF{\cdot}Al_2O_3{\cdot}3SiO_2$	1.4–1.9
Zinnwaldite $LiF{\cdot}KF{\cdot}FeO{\cdot}Al_2O_3{\cdot}3SiO_2$	1.2–1.3
Petalite $Li_2O{\cdot}Al_2O_3{\cdot}4SiO_2$	1.6–2.2
Amblygonite $2LiF{\cdot}Al_2O_3{\cdot}P_2O_5$	3.5–4.2
Eucryptite $Li_2O{\cdot}Al_2O_3{\cdot}2SiO_2$	2.3–3.3
Jadarite $Na_2O{\cdot}Li_2O{\cdot}2SiO_2{\cdot}3B_2O_3{\cdot}H_2O$	~0.1
Hectorite $Na_{0.3}(Mg,Li)_3Si_4O_{10}(F,OH)_2{\cdot}nH_2O$	~0.4
Soils	
Earth	13–22 ppm
Moon	11–14 ppm
Mars	1.8–3 ppm
Brines	
Salar	20–1500 ppm
Geothermal	0.3–440 ppm
Oilfield	50–572 ppm
Water	
Marine	0.1–1.2 ppm *
Fresh	0.001–0.02 ppm
Deep-sea or submarine	
Fe–Mn nodules	20–300 ppm
Fe–Mn crusts	1–1200 ppm
Li–ion batteries	11
World Coals	1–80 ppm
Coal tailings	
Gangue	420–550 ppm
Fly ash	70–650 ppm
Bottom ash	46–146 ppm

* 12–21 ppm in Dead Sea water [20].

Geothermal brines [17,33,34] and seawater [20,34,35] are likely to be considered economically viable for utilization in the future. Extensive deposits of ferromanganese crusts and nodules beneath the oceans may also serve as potential sources of lithium, as some deposits located near hydrothermal systems are notably rich in this element [17,21]. Several research studies are likewise looking towards extraterrestrial bodies as potential lithium

reservoirs [22,23], and space exploration is currently experiencing dynamic growth (NASA's Artemis Program of lunar exploration) [36].

Alternatively, various secondary materials (Table 1) have been explored as valuable resources of lithium [17,18,34]. Among these, spent lithium-ion batteries are the most extensively studied, with laboratory tests showing very high lithium recovery efficiencies [37–39], while the actual lithium recycling rates of existing technologies (e.g., TOXCO, Accurec GmbH) remain unavailable [24]. Wastewaters (i.e., oilfield brines) generated during oil, gas, and shale gas operations have also been identified as potentially important sources of lithium, as they can contain up to a few hundred ppm Li^+, depending on the region [25,26,40,41].

In recent times, researchers have assessed unconventional sources of lithium, such as coal and coal tailings, like coal gangue, coal fly ash, and coal bottom ash [27–29]. Although these materials have lower lithium contents compared to ores (Table 1), the levels appear sufficient to target them for lithium recovery. Therefore, the purpose of this paper is to provide an overview of the potential for recovering lithium from these unusual sources, especially since resource diversification is of great interest to global industry.

2. Methodology

The literature search was conducted in May–August 2024 using two primary databases: Web of Science and Scopus, along with databases from specific publishers (ACS—American Chemical Society, IOP Science, MDPI, Royal Society of Chemistry, Taylor & Francis Online, ScienceDirect, SpringerLink, Wiley Online Library) as well as freely available online papers, statistical data, and institutional sources. The search focused on the variation of key terms, particularly lithium, coal, coal gangue, coal fly ash, coal bottom ash, recovery, and leaching, among others. Although no strict restrictions were placed on the publication date, the search was inherently limited by the availability of each database.

Research articles and reviews were methodically identified by assessing both the titles and content of the papers. Additionally, efforts were made to ensure a comprehensive coverage of the relevant literature, including cross-referencing citations and reviewing supplementary materials where applicable. Each publication was carefully reviewed on an individual basis to exclude those that did not contain relevant information on lithium. Special attention was paid to the methodological approaches, key findings, and relevance of the studies to the current research context. In total, 160 references were selected that aligned with the objectives and requirements of this literature review, providing a robust foundation for further analysis and discussion.

However, it should be noted that English-language literature does not fully encompass the available data on the occurrence and recovery of lithium from coal and its by-products, as this topic has also been explored in some Chinese-language publications. Unfortunately, these papers were not included in the following review due to language barriers and accessibility limitations, which prevented a thorough examination of their content.

3. Lithium in Coal

3.1. Lithium-Rich Coal Seams

Lithium was detected in coal long before it became a critical material [30]. However, over the past two decades, exploration has focused on identifying deposits enriched in this element [27]. Ketris and Yudovich [42] reported that the average lithium content in coal worldwide is 12 ppm, and in brown and hard coal, it is 10 ± 10 ppm and 14 ± 1 ppm, respectively. Nevertheless, there are numerous coal beds with remarkably high concentrations of potentially recoverable lithium [27], reaching up to several hundred ppm. Table 2 shows ranges of lithium concentration in coals from various countries, but it should be emphasized that these values are indicative, as they depend on the location of the mines, the type of coal seams, the depth of coal sampling, the analysis method used, and number of representative samples analyzed, etc.

Table 2. Lithium concentrations in lithium-bearing coal deposits in various regions [27,29,43–60].

Country	Lithium Concentration, ppm
Australia	8–34
China	28–264
India	26–353
Russia	27–172
South Africa	45–81
Turkey	1.2–140
United States	6–185

China is the world's largest consumer of lithium [9] and producer of coal (Figure 2) [61]. Hence, it is not surprising that many scientists have intensively studied China's coal deposits for their high lithium content [43–51,62–66]. Coals with extra-high (above 120 ppm) and high (50–120 ppm) lithium content [44] have been found in Inner Mongolia (Jungar mining area and Zhuozi Mountain mining field [45,46]), Shanxi Province (Pingshuo mining district, Jincheng and Xishan coalfields [44,47–49]), Chongqing (Nantong mining area [62], Guangxi Province (Fusui coalfield [44]), and Henan Province [43]. In such coals, average lithium levels range from 113 ppm to 286 ppm, but in some areas, maximum lithium contents as high as 566–657 ppm (Jungar coalfield) or 840 ppm (Pingshuo mining area) have been reported [43,44]. High-lithium (90–1099 ppm) minerals (tonsteins, tuffs) were also found in some coals of the Songzao coalfield (Chongqing) [67]. It is estimated that the Jungar coalfield alone contains approximately 3 million tons of lithium resources [44], while lithium reserves in the Ningwu coalfield amount to 558,000 tons [48]. For Chinese coals, Sun et al. [63] proposed to take 80 ppm Li as the minimum mining grade and 120 ppm Li as the mining grade (economic grade). However, recently [44,66], an average value of 50 ppm Li in coal seams has been reported as meeting requirements for its extraction.

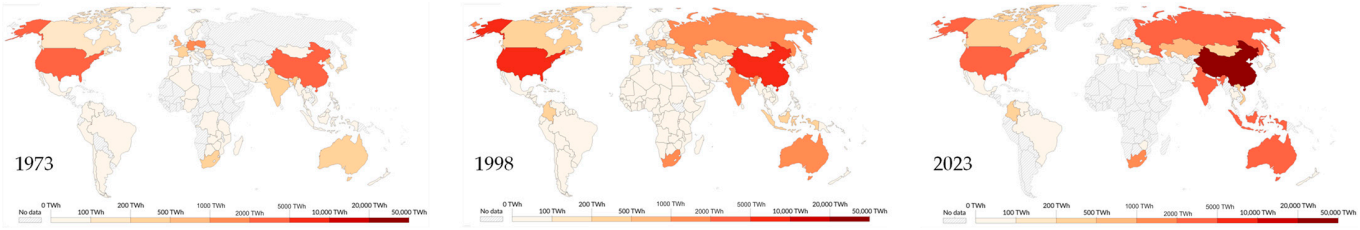


Figure 2. Global changes in coal production over the last fifty years: coal production levels (in TWh) by country in 1973, 1998, and 2023 [68].

High-lithium deposits were identified in coal basins in the Russian Far East [50,55]. These are located in Krylovsk and Verkhne–Bikinsk areas with Cenozoic host- and basement rocks out the coal seams containing up to 0.1%–0.3% Li. In coarse-grained sediments of these deposits, lithium is concentrated in the clay cement of the host rocks. Much more enriched sources have been found in Partizansk coalfields bearing up to 1% Li in argillized basaltic sills [50]. Recently, Arbuzov et al. reported the occurrence of 28–172 ppm Li in germanium-bearing coal seams of the Spetsugli deposit in the Pavlovsk coalfield [55], but only 5–22 ppm Li in coals of the Sakhalin island [69].

Third-world coal-based sources of lithium have been indicated in the United States [52, 57–59]. The average lithium content in the American coals is 11–16 ppm, although a range of minimal and maximal values detected is 0.2–374 ppm [52]. Lehmden et al. [70] compared the concentration of trace elements in different coal samples, but lithium (0.3–300 ppm) was reported only for some of them. Finkelman et al. [57] found that the concentration of lithium in bituminous coals is considerably higher (44 ppm) than in the lower-rank (sub-bituminous) coals (6 ppm). Li et al. [52] stated that bituminous coals from the southern Appalachian region have relatively high probabilities of being promising sources of lithium. Total reserves of lithium in U.S. coals have been estimated at about 2.7 million metric tons,

but only 1.8% of the coal samples can meet the minimum cut-off grade of 80 ppm proposed by Sun et al. [63].

Other countries are also beginning to pay more attention to the lithium content of their coal deposits. For example, Das et al. [60] reported lithium levels in some coals in India, the world's second coal producer in 2023 [61]. The samples were collected from different coalfields in the Central, Eastern, and Northeastern parts of the country. These were Gondwana coals from the Talcher Valley, Ib, Wardha, Rajmahal, and Korba coal mining areas, and Eocene coals from the Makum coalfield in Assam. Lithium concentrations in the Gondwana coals (bituminous and sub-bituminous) were in a range of 23–353 ppm (mean: 117 ppm) and were lesser than in the Eocene coals (26–761 ppm, mean 390 ppm). The richest coal deposits were found in the Wardha Valley (mean: 353 ppm Li) and Jaintia Hills (mean: 761 ppm Li). Coals from South Africa (ranked seventh in coal producers worldwide [60]) have relatively high lithium concentrations (45–81 ppm Li) [54]. Turkish coals from Kangal in Central Anatolia show 25–40 ppm Li [71], but Palmer et al. [56] performed more detailed studies of coals originating from various regions of Turkey. They reported lithium contents in a range of 1.2–140 ppm, and the highest concentrations were found in coals from two regions, i.e., Marmara South (up to 110 ppm) and Aegean (up to 140 ppm). Querol et al. [72] studied elemental composition in different density fractions of Spanish coal with an average lithium content of 74 ppm. The lithium levels were in a range of 12–169 ppm, but the most enriched fractions were two of them with densities in a range of 2.2–2.6 g/cm^3.

3.2. Lithium Determination in Coal

Lithium is an element of low atomic mass, thus its accurate analysis in coal samples can be affected by many factors, i.e., sample preparation, analytical method used, etc. leading to some scatter of the results [70]. There is not one standard procedure for lithium determination, but some practical remarks can be found in the papers. For example, Qin et al. [27] discussed shortly applicability of various analytical methods in coal analysis. These were spark source mass spectrometry SSMS, particle-induced γ-ray emission PGE, X-ray fluorescence XRF, ultraviolet–visible spectrophotometry UV–VIS, flame photometry, and atomic absorption spectrometry AAS. The main disadvantages of some methods are their unsuitability for light elements (XRF), detection limits, or a lack of suitable lithium-sensitive chromogenic reagents (UV–VIS) [70].

Coal samples are typically crushed and homogenized to ensure the representativeness of the subsample, often ashed carefully to prevent losses due to volatility, and then dissolved in mineral acids. Coal combustion for analytical purposes eliminates organic matter, reduces sample complexity, and converts lithium into a soluble, measurable form, ensuring reproducibility and accuracy of the analysis. Alternatively, sequential digestion in concentrated mineral acids (e.g., HF, HCl, HNO_3, and aqua regia) is used. Acid digestion methods are particularly effective, ensuring the complete transfer of lithium to the liquid phase in a fast, safe, and simple manner with minimal contamination and low reagent consumption. Wet digestion also generates minimal amounts of waste, as it effectively dissolves refractory minerals and decomposes organic matter.

The concentration of metal ions in the resulting solutions is determined usually using inductively coupled plasma mass spectrometry ICP–MS or inductively coupled plasma atomic emission spectrometry ICP–AES (also: inductively coupled plasma optical emission spectrometry ICP–OES). These methods are considered routine and reliable due to their high selectivity, sensitivity, and low detection limits (0.012–0.5 ppm for ICP–MS and 0.013 ppm for ICP–AES [27,73]). Some procedures used for coal sample preparation are shown in Figure 3.

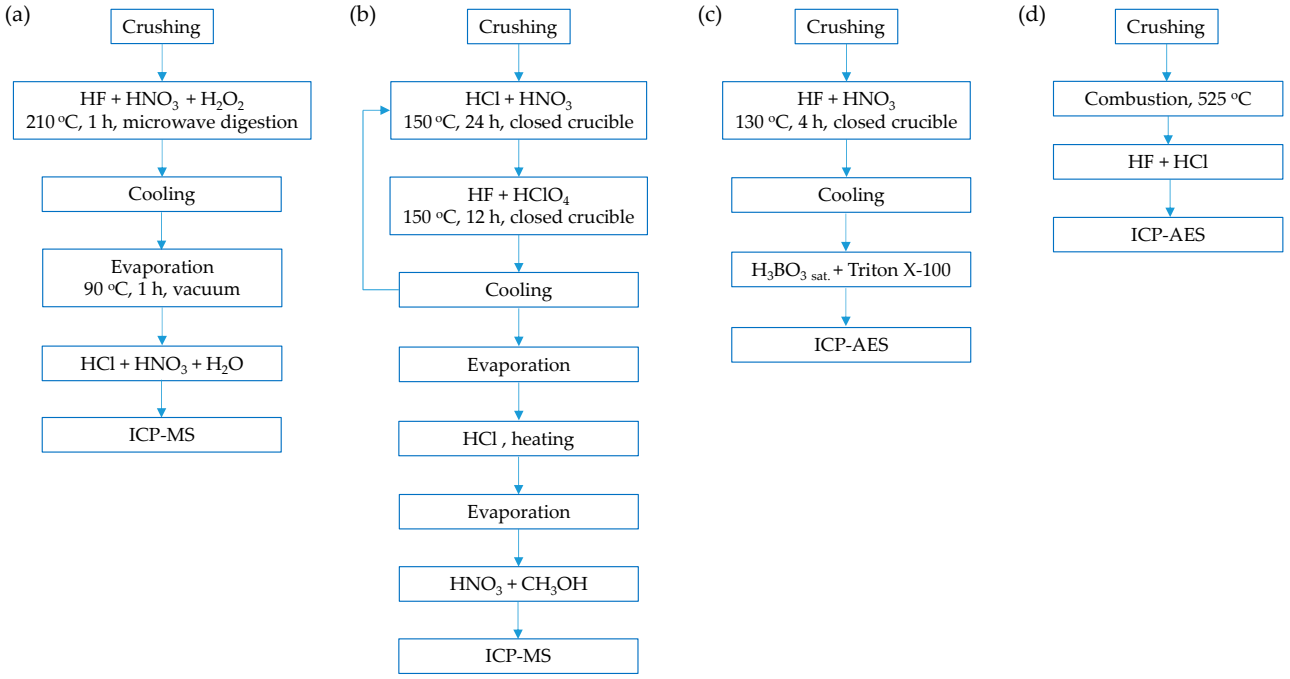


Figure 3. Schemes of coal dissolution for lithium quantitative analysis: (**a**) [48], (**b**) [51], (**c**) [54], and (**d**) [74].

Instrumental techniques for lithium analysis are currently used as standard procedures. Although lithium is relatively easy to determine in aqueous solutions, careful preparation of solid samples and precise measurement conditions are essential to avoid experimental errors. These include the proper selection of solvents for effective coal sample dissolution, background correction, accurate apparatus calibration, and protocols involving the use of standards to address interference effects from other elements (e.g., Na, K, and Ca) present in the analyzed sample [73].

3.3. Occurrence Modes of Lithium

The lithium analysis procedure is often correlated with the modes of metal occurrence in coal. This is essential not only for the geochemical characterization of the coal beds but also for assessing their potential as a valuable source of lithium, as well as other elements such as rare earth metals, gallium, germanium, etc. [29,30,47,50,75–77]. The elements can be associated with inorganic substances (minerals or non-crystalline metalloids) or organic matter in coal, either chemically or physically bound. They may also occur in pore water or be adsorbed on the surface of organic particles. Various methods are used to investigate the modes of element occurrence in coal [75], but sequential leaching procedures are most commonly employed for quantitatively determining the types of lithium-bearing minerals.

Finkelman et al. [57] conducted selective leaching of coals (bituminous with 44 ppm Li, sub-bituminous with 6 ppm Li) from the USA or not (unknown sources). They used subsequently the following solvents (each stage was conducted for 18 h): 1 M CH_3COONH_4 for the removal of exchangeable cations, 3 M HCl to dissolve carbonates and monosulfide-associated cations, 48% HF to remove silicates associated cations, and 2 M HNO_3 to extract disulfide-associated cations. It was found that HF leached 65%–95% Li from high-rank coals, but 15%–90% Li from low-rank coals. CH_3COONH_4, HCl, and HNO_3 removed relatively small amounts of lithium. The solvents removed 70%–95% Li from high-rank coals, but 15%–100% from low-rank coals. Thus, they suggested that in most high-rank coals about 90% of lithium was associated with clays and micas (silicates), while the remainder were associated with organic matter or acid-insoluble phases (e.g., tourmaline). In low-rank coals, about 30% of lithium could be organically bounded, while 70% with silicates.

A similar procedure was used by Wang et al. [76] to determine the modes of lithium occurrence in bituminous coals (33–368 ppm Li) from Qinshui Basin (China), indicating its association with clay minerals such as kaolinite and illite. However, they observed a gradual increase in the lithium holding capacity of clay minerals from the roof and floor, parting to coal. This behavior has been attributed to the presence of humic acid.

Zhang et al. [58,59] used another procedure for the sequential chemical extraction of lithium from coal of different density fractions (150 or 185 ppm Li) sourced from western Kentucky (USA). The solid sample was subsequently treated with the following solutions: 1 M $MgCl_2$ to determine ion-exchangeable lithium, 1 M CH_3COONa to dissolve carbonates, 0.04 M $NH_2OH{\cdot}HCl$ to dissolve metal oxide, concentrated HNO_3 with H_2O_2 and 1 M CH_3COONH_4 in 20% HNO_3, both for acid soluble compounds, and, finally, acid digestion to determine insoluble fraction. They found that 91% of lithium occurred as insoluble forms that were not dissolved even under strong acidic and oxidizing environments. This was explained by the association of the element with the clay minerals. Positive effects of former coal calcination (600–900 °C) on lithium leaching were attributed to dehydration and disintegration of kaolinite and dehydroxylation and expansion of muscovite/illite.

Sun et al. [48] determined six modes of lithium occurrence in coals (156 ppm Li) from the Ningwu coalfield (China). These were determined in the following sequence: water-soluble (H_2O, 25 °C, 24 h), ion exchangeable (CH_3COONH_4, 25 °C, 24 h), organic bonded ($CHCl_3$, then the floating part dried, ashed, and treated with HNO_3 + $HClO_4$, 200 °C, 60 h), carbonate (HCl), silicate ($CHBr_3$, then the floating part dried, ashed, and treated with HNO_3 + HF, 200 °C, 60 h), sulfide (HNO_3, 5 h). They found that lithium in the investigated samples existed mainly in the silicate fraction (82.8%), but it was also related to sulfide (11.4%) and organic matter (5.5%).

Most of the literature data indicate that the enrichment of lithium in world coals is associated with minerals, mainly silicates, and aluminosilicates, rather than organic matter [44,76]. However, Lewińska-Preis et al. [74] reported for two Norwegian low-lithium coals (0.4–5 ppm) different lithium affinity, depending on the coal mine (Spitzbergen). Total lithium associated with minerals was found in Kaffiorya's coal (up to 23 ppm Li), while most lithium showed high affinity to organic matter in Longyearbyen's coal (7–107 ppm Li). Modes of lithium occurrence in other coals are shown in Table 3.

Table 3. Modes of lithium occurrence in some coals [27,44,50,66,78,79].

Region/Coalfield	Lithium-Bearing Minerals
Bulgaria	
Pernik	organic matter
China	
Jungar	aluminosilicates, chlorite, kaolinite, boehmite, chamosite
Ningwu	kaolinite, chlorite, boehmite
Jingchen	Cookeite
Chongqing	kaolinite
Shuicheng	aluminosilicates
Xingren	clay minerals, organic matter
Russia	
Bikinsk	clay minerals, tosudite

3.4. Lithium Extraction

Although coal is considered a source of lithium recovery and minimal cut-off grades have been proposed, there is no technology for metal extraction. Recently, Li et al. [66] developed a theoretical model for the cooperative exploration of the coal–lithium deposit (116 ppm Li, Jungar coalfield) from the perspective of technical optimization and economic rationality, but without strict attention to lithium production from the raw material.

Laboratory studies on direct lithium extraction from coal are also in their infancy. Zhang et al. [58,59] leached raw and calcined (400–900 °C, 2 h, static air conditions) coals from western Kentucky (USA) in HCl solution (1.2 M, 75 °C, 300 min, 10 g/L). Lithium

leachability from the coal was very low, i.e., 3%–10%. The calcination of the material improved lithium extraction to a maximum of about 80% for a calcination temperature of 600 °C. A further increase in the calcination temperature reduced lithium dissolution to 10%–20%. Kinetic analysis of the acid leaching showed that the process was controlled by interface transfer and diffusion across the product layer. The hindrance of lithium leaching from the sample calcined at 900 °C was correlated with the recrystallization and sintering of clays, which formed a thick blocking layer.

4. Recovery of Lithium from Coal Gangue

4.1. Coal Gangue

World coal production and consumption have increased significantly over the last twenty-five years, driven primarily by China, although in some regions, such as Europe or the USA, they have slowly decreased due to the diversification of energy sources [80]. Coal mining is inevitably associated with the production of large amounts of waste. These are generated at various stages of the coal mining and washing processes, with coal gangue (Figure 4) being the most predominant form of solid waste, accounting for 10%–20% of the total output of raw coal, and even reaching 30%–40% in some coal mines [81–85].

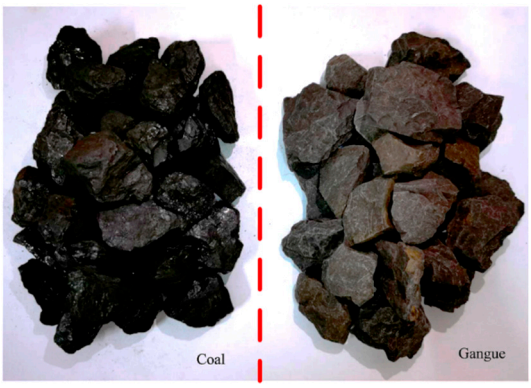


Figure 4. Coal and coal gangue [86].

Coal gangue is a black–gray shale rock with lower carbon content, harder than coal. Due to its poor calorific value, large sluggishness, and some problems with its complete utilization (e.g., in the production of building materials, as roadbed filler, electricity generation), it is typically stockpiled in exposed to weathering heaps, waste dumps, discarded on the surface near the mine [82]. For example, it is estimated that coal gangue in China has exceeded six billion tons accumulated in 1500–1700 large-scale waste heaps occupying over 13,300 ha [83]. The disorderly accumulation of coal gangue not only takes up a large amount of ground space but can also spontaneously combust and explode, cause landslides, emit harmful gases and dust, and release heavy metals and acidic water, thereby polluting the surrounding ecological environment [81,87–90]. However, abnormally high concentrations of lithium in such coal by-products [28,91–93] provide a new opportunity for their comprehensive use. Consequently, coal gangues derived from Chinese sources have been the most intensively studied for their lithium recovery potential [94–102].

Coal gangue contains 10%–30% of carbon, but its composition is generally dominated by oxides, i.e., 30%–70% SiO_2, 13%–40% Al_2O_3, up to 15% Fe_2O_3, and others like CaO, MgO, TiO_2, K_2O, Na_2O, and MnO, occurring usually at a few percentage levels [82,88]. The mineral composition of coal gangue involves mainly quartz, kaolinite, pyrite, boehmite, mica, dickite, and anatase [28,85,91–94,96,98–103]. There are also identified a range of heavy metals like Zn, Cr, Zn Pb, As, Hg, and some valuable elements like Ga, Nb, Ce, La, Y, etc. [28,90–93,103].

4.2. Occurrence Modes of Lithium

Chinese coal gangue is enriched in lithium, with its concentration being significantly higher than in coal (Table 4). Lithium in coal gangue exists mainly as silicates and aluminosilicates, predominantly in the form of kaolinite [28,91–104]. Since metal ions are strongly bonded by aluminosilicates, there is no possibility of directly leaching lithium from the raw materials. The removal of excess carbon and destruction of the lithium mineral carriers are key factors affecting lithium release from the coal gangue, similar to coal.

Table 4. Lithium occurrence in Chinese coal gangues.

Source	Concentration, ppm	Bearing Minerals	Ref.
Thermal coal preparation plant, Jungar	421	Kaolinite	[28]
Malan coal mine, Shanxi Province	110	Kaolinite	[92]
Antaibao coal mine, Shanxi Province	100	Mica, clay	[93]
Shuozhou, Shanxi Province	160	No details	[94]
Heidaigou open-pit coal mine	107	Kaolinite	[95]
Zhuneng coal preparation plant, Jungar	437	Clay minerals	[97]
Guangxi Province	511 *	Inorganic matter	[98]
Xian'an coalfield, Guangxi Province	550	Aluminosilicates	[99]
Jincheng coal seam, Shanxi Province	277	Clay minerals	[100]
Thermal coal preparation plant, Jungar	223	Kaolinite	[101]
Guangxi Province	550	Kaolinite	[102]
Pingshuo coal mine, Shanxi Province	344	Kaolinite	[103]
Pingshuo coal gangue power plant, Shanxi Prov.	121	Kaolinite, quartz	[104]

* Recalculated from 0.11% Li_2O.

Chen et al. [28] performed sequential chemical extraction of lithium from coal gangue using a variant of the Tessier procedure (originally, the solid residue was digested with a mixture of HF and $HClO_4$ concentrated acids (5:1) [105]), as shown in Figure 5a. The speciation identified five forms of lithium occurrence: exchangeable (e.g., ions adsorbed on clays, hydrated iron and manganese oxides, humic acids), bound to carbonates, bound to iron and manganese oxides, bound to organic matter (e.g., associated with humic or fulvic acids or bioaccumulated), and residual. The residual solid primarily contains primary and secondary minerals, which may hold trace metals within their crystal structure. These metals are not expected to be released into solution over a reasonable time span under typical environmental conditions. It was found that most of the lithium (91%) was present in the residual fraction (i.e., silica–aluminate minerals), with much smaller amounts in the iron–manganese oxides and organic matter fractions. A similar result (95.8% lithium in clay minerals) was reported for another sample of coal gangue, though with a lower lithium concentration [101].

Qin et al. [95] adopted the BCR sequential extraction method (proposed by the Commission of the European Community Bureau of Reference [106]) to analyze the lithium occurrence modes in the coal gangue samples (Figure 5b). Four categories were considered, i.e., acid-soluble, reducible (e.g., iron–manganese oxides), oxidizable (e.g., organic matter and sulfides), and residual. It was found that almost all lithium existed in the residual fraction, while only traces were attributed to the oxidizable category [95]. It was concluded that lithium likely occurs in the kaolinite facies.

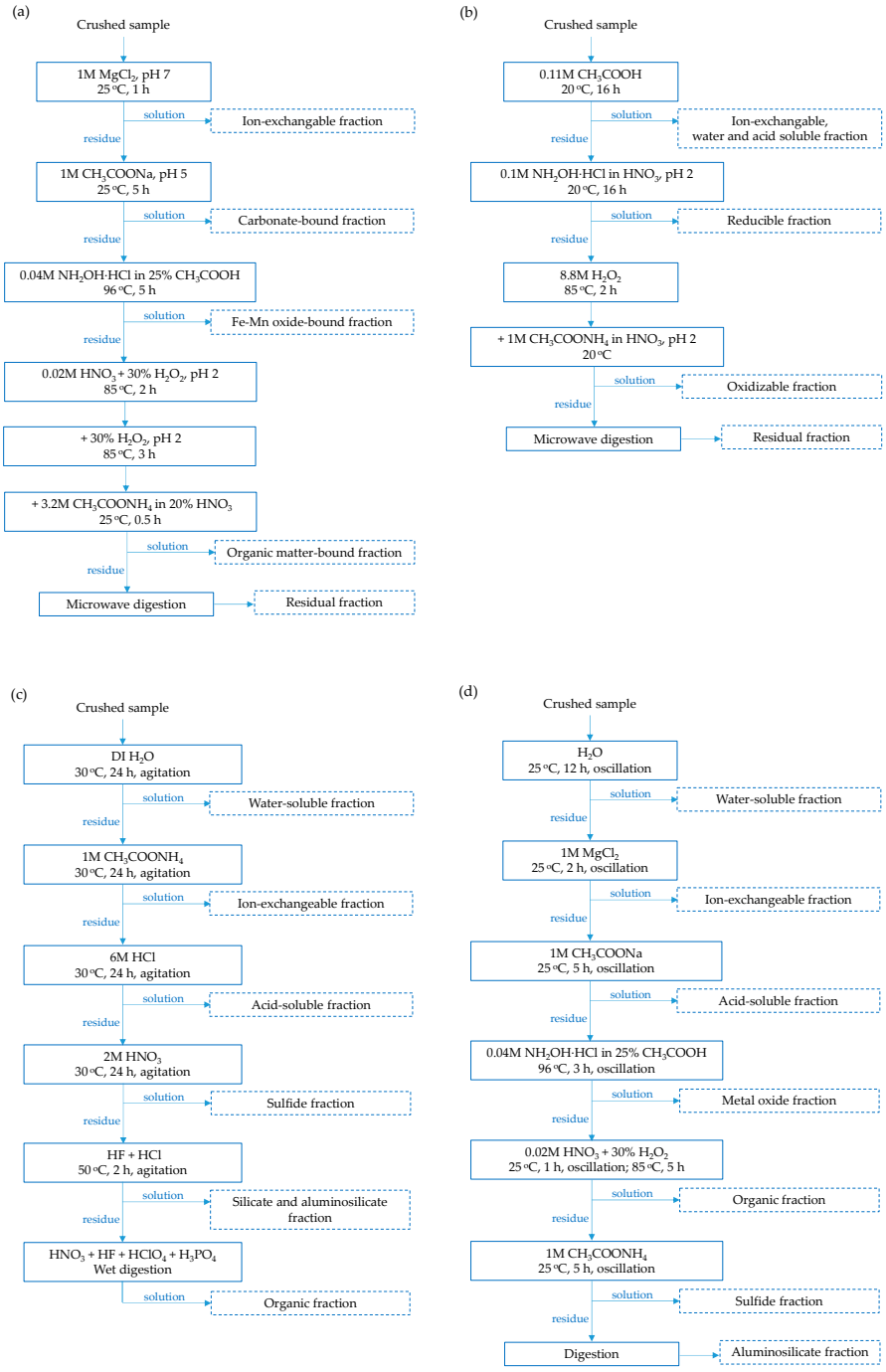


Figure 5. Schemes of sequential chemical extraction of lithium from coal gangue: (**a**) variant of the Tessier method [28], (**b**) the BCR method [106], (**c**) combined method [100], (**d**) seven-fraction procedure [99].

Kang et al. [100] combined two methods used by other authors (Figure 5c). The presence of metals in coal gangue was classified into six chemical forms: water-soluble, ion-exchange, acid-soluble (carbonate, sulfate, phosphate, etc.), sulfide, silicate, aluminosilicate, and organic. They confirmed that most of the lithium (94.5%) is found in the silicate and aluminosilicate fraction (within clay minerals), while the remaining lithium was attributed to acid-soluble (3.1%) and organic (1.6%) forms.

A more detailed analysis was performed by Xie et al. [99], who investigated the distribution of lithium in seven fractions of coal gangue (Figure 5d). These fractions included water-soluble, ion-exchange, acid-soluble, metal oxide, organic, sulfide, and

aluminosilicate forms. Consistent with earlier studies, almost all lithium (98.9%) was found in the aluminosilicate fraction, primarily within silicate clay minerals. The proportion of lithium in the oxidized form was very low (0.4%), while only trace amounts of lithium were detected in the remaining fractions.

4.3. Lithium Pre-Enrichment Methods

Lithium distribution was also correlated with coal gangue fractions of different particle sizes and densities [28,101,104]. Ma et al. [104] found that larger particles, greater than 5 mesh (comprising 3% of the particle size distribution), were significantly enriched in lithium compared to finer particles (Figure 6), while the dominant fraction (67%) of particle sizes was 5–40 mesh.

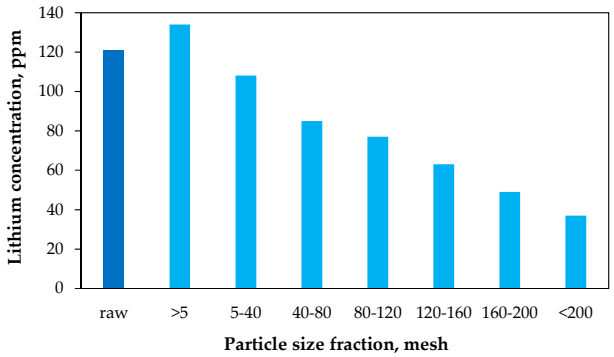


Figure 6. Lithium concentration in coal gangue and its particle fractions [104] (5 mesh~4 mm; 200 mesh~0.07 mm).

A similar tendency in lithium accumulation was reported by Chen et al. [28], who found that lithium concentration decreased with decreasing particle size, from 519 ppm for particles larger than 0.25 mm to 374 ppm for a fraction below 0.075 mm. The smallest particle fraction contained the highest proportion of total lithium (43%), while this proportion decreased with increasing particle size. Lithium was significantly enriched (by 1.23 times) in the middle-density fraction (2.4–2.6 g/cm^3), particularly in fractions with the same density as kaolinite (2.54–2.60 g/cm^3). Therefore, physical separation to enrich lithium and its graded extraction from different fractions was proposed. This involved extracting lithium from large particles (above 0.125 mm) or co-extraction with niobium (0.125–0.075 mm or density fractions higher than 2.2 g/cm^3), and using the remaining fractions for power generation, followed by metal extraction from the resulting coal fly ash.

Comparable results were presented by Zhang et al. [91]. They observed an increased mass yield of the particle fractions as particle size decreased from 0.25–0.5 mm to below 0.075 mm. The highest lithium content, around 465 ppm (an enrichment of 1.06 times), was found in two fractions of larger particle sizes, above 0.125 mm. The density fraction of 2.4–2.6 g/cm^3 exhibited the highest mass yield and lithium concentration (514 ppm).

Dai et al. [93] performed sorting experiments for the pre-enrichment of lithium (and gallium) based on the element occurrence in coal gangue. The material was composed mainly of mica, quartz, pyrite, and clay. Mica and clay were identified as lithium carriers, as determined by a six-step sequential chemical extraction procedure similar to that described earlier by Sun et al. [48]. The coal gangue (100 ppm Li) was first distributed in a single layer using a vibrating feeder [93]. As the coal gangue fell, an XRF sensor captured and analyzed its fluorescence, identifying material with element content higher than or equal to the threshold value, followed by directing these material fractions into a tailings bin via an electromagnetic hitter. Particles with elemental contents lower than the threshold concentration were collected in a concentrate bin through natural fall. After the sorting, the concentrate yield was 68.8% with a lithium concentration of 194 ppm, while the Li concentration in the tailings was about 23 ppm. Thus, subsequent lithium extraction can be simplified, resulting in reduced production costs.

Fang et al. [103] proposed flotation as a pre-enrichment stage for lithium extraction. They found that the main minerals in coal gangue are kaolinite, quartz, and pyrite, with lithium (344 ppm) primarily associated with kaolinite and other clay minerals. The flotation tests were conducted in a single-cell laboratory flotation machine (1 L, 80 g/L, natural pulp pH, 1800 rpm, aeration 0.1 m^3/h, 3 min) using diesel oil as the collector and sec-octanol as the foaming agent. The results showed that most of the lithium was collected in the tailings, where the lithium content was enriched by a factor of 1.02 compared to the original sample, and the recovery rate of the carrier minerals of lithium reached about 66%. The authors suggested that the remaining tailings could be dissociated and re-floated, reducing grinding time and saving costs.

4.4. Lithium Extraction

Understanding the state of lithium in coal gangue is essential for effective hydrometallurgical extraction. Kaolinite, a primary lithium carrier, exhibits good resistance to water, acids, and alkalis under normal temperature and pressure conditions. Consequently, coal gangue demonstrates low activity and efficiency during leaching. For example, Chen et al. [28] reported that only about 5.8% of lithium was extracted from coal gangue during leaching in 3 M HCl at an elevated temperature (90 °C, 3 h). Zhang et al. [91] showed maximal 2.5% lithium extraction from different particle and density fractions of coal gangue using 2 M HCl (60 °C, 4 h). Practically no lithium dissolution was observed in 15% H_2SO_4 (30–90 °C) [102]. Similarly, direct or grind (in a planetary ball mill) leaching of coal gangue in ammonium salts (chloride and/or sulfate) solutions was ineffective in terms of lithium dissolution [95]. Therefore, an activation stage is necessary for further successful hydrometallurgical recovery of lithium (Table 5).

Table 5. Optimal conditions of lithium recovery from coal gangue (lithium concentration in the feedstock is shown in Table 4, according to the references).

Pretreatment Stage	Leaching Conditions	Lithium Extraction	Ref.
One-step pretreatment			
Calcination			
600 °C, 2 h	3 M HCl, 90 °C, S/L 1:10, 3 h, 200 rpm	92.0%	[28]
400 °C, 0.3 h	2 M HCl, 60 °C, S/L 1:10, 4 h, 200 rpm	94.3%	[97]
500 °C, 1 h	15% H_2SO_4, 90 °C, S/L 1:5, 0.7 h, stirring	99.6%	[102]
650 °C, 2 h	6 M H_2SO_4, 120 °C, S/L 1:10, 1 h, 400 rpm	74.5%	[100]
550 °C, 0.5 h	HNO_3, 150 °C, S/L 1:5, 2 h, 400 rpm	80.5%	[94]
500 °C, 2 h	8 M $H_2C_2O_4$, 90 °C, S/L 1:5, 1 h, stirring	89.1%	[98]
Roasting			
$(NH_4)_2SO_4$ + NH_4Cl, 400 °C, 1 h	H_2O, 60 °C, 1 h, shaking	80.8%	[95]
Baking			
70% H_2SO_4, 180 °C, 1 h	H_2O, 25 °C, S/L 1:5, 1 h, stirring	84.4%	[99]
Intercalation			
DMSO, 60 °C, 24 h	3 M HCl, 90 °C, S/L 1:10, 3 h, 200 rpm	17.6%	[28]
Multi-step pretreatment			
I. Intercalation CH_3COOK, 25 °C, 28 h II. Delamination H_2O, 0.5 h, ultrasound; drying III. Roasting $(NH_4)_2SO_4$, 380 °C, 1 h	H_2O, 70 °C, S/L 1:80, 1 h, stirring	86.6%	[96]
I. Grinding 1.5 h, ball mill II. Thermal activation N_2 atmosphere, 400 °C, 0.5 h	0.2 M $(NH_4)_2SO_4$, pH 1, 60 °C, S/L 1:30, 3 h, 500 rpm	84.8%	[101]

Calcination (in air conditions) is a common method used to convert kaolin and destroy its lattice structure. This effect is attributed to the transformation of kaolinite into metakaolinite as a result of losing hydroxyl groups (i.e., from structural and interlayer water) [94,100]:

$$Al_2O_3 \cdot 2SiO_2 \cdot 2H_2O \rightarrow Al_2O_3 \cdot 2SiO_2 + 2H_2O \quad \text{at 450–850 °C} \quad (1)$$

followed by the destruction of silicon–oxygen tetrahedrons:

$$Al_2O_3 \cdot 2SiO_2 \rightarrow Al_2O_3 \cdot (2\text{-}x)SiO_2 + xSiO_2 \quad \text{at 850–950 °C} \quad (2)$$

and metakaolinite decomposition:

$$Al_2O_3 \cdot (2\text{-}x)SiO_2 \rightarrow \gamma\text{-}Al_2O_3 + (2\text{-}x)SiO_2 \quad \text{at 950–1100 °C} \quad (3)$$

At higher temperatures, metastable (amorphous) SiO_2 converts into mullite:

$$3\gamma\text{-}Al_2O_3 + 2SiO_2 \rightarrow 3Al_2O_3 \cdot 2SiO_2 \quad \text{above 1100 °C} \quad (4)$$

and cristobalite:

$$SiO_2 \rightarrow SiO_{2\,c} \quad \text{above 1200 °C} \quad (5)$$

Structural changes occurring in coal gangue under different temperature conditions are analyzed using various diagnostic methods, including X-ray diffractometry XRD, Fourier transform infrared spectrometry FTIR, thermogravimetric analysis TGA, and differential scanning calorimetry DSC [94,100]. X-ray diffraction, a versatile and non-destructive analytical technique, is used to analyze the phase composition, crystal structure, and orientation of the minerals present in the material. It has been observed that the intensity of kaolinite diffraction peaks weakens and eventually disappears as the temperature increases from 400 °C to 700 °C, indicating its gradual decomposition. This is further correlated with FTIR spectra, where the absorption bands associated with O–H stretching vibrations and the absorption peaks of Al–O–H vibrations disappear at 500 °C due to kaolinite dehydroxylation and its transformation into metakaolinite. Simultaneously, absorption bands corresponding to Si–O vibrations merge into a single band and shift to a shorter wavelength position due to the increased ordering of the silicate structure. TGA and DSC measurements, in turn, allow for the detection of mass loss and identification of exothermic and endothermic phase transformations, respectively. These can be then attributed to the combustion of volatile matter and fixed carbon, as well as the generation of mullite and the dehydroxylation of kaolinite. The experimental results can also be correlated with thermodynamic calculations, providing additional support for predicting possible reactions during the thermal treatment of the coal gangue.

Calcination decomposes organic matter in coal gangue and removes some volatile compounds, which simultaneously increases the lithium concentration in the calcined products. Zhang et al. [91] reported an enrichment factor of approximately 1.3 for calcination temperatures ranging from 400 °C to 950 °C. This process also exposes lithium for ion exchange and enhances the dissolution of minerals during subsequent leaching. For example, leaching of roasted coal gangue (500 °C) solely with water resulted in 12% lithium extraction [102].

A significant increase in lithium leaching in 3 M HCl, from a few percent up to 92%, was observed after calcination of coal gangue at 600 °C [28]. Acid leaching of calcined fractions with different particle sizes also showed that lithium extraction slightly increased from 87.8% to 93.7% as the particle diameters decreased from larger than 0.25 mm to 0.125 mm and smaller. This increase was attributed to the change in the surface area of the powdered samples.

Roasting of coal gangue followed by leaching in hydrochloric acid was also examined by Zhang et al. [91,97]. They observed a significant improvement in lithium leachability (2 M HCl, 60 °C, 4 h) from the calcined product compared to the raw material. However, leaching efficiency decreased from 70% to 25% as the calcination temperature increased from 400 °C to 950 °C [91]. An acceptable lithium leaching rate was achieved at a roasting temperature of 400 °C (about 80% in 3 M HCl, 90 °C, 3 h) [97]. Further optimization of the parameters revealed that lithium extraction is slightly dependent on roasting time (ranging from 20 to 180 min), acid concentration (ranging from 2 to 7 M), and leaching temperature (ranging from 60 to 150 °C), but strongly affected by the leaching duration (30 to 240 min). This behavior was explained by changes in the coal gangue during roasting, which involved the disappearance of boehmite, a partial transformation of kaolinite into metakaolinite, and the combustion of internal carbon, leading to an expansion of porosity and an increase in specific surface area. Kinetic analysis of the lithium dissolution, according to the shrinking core model, showed that diffusion through the solid layer (especially kaolinite) was the rate-determining step.

Xie et al. [102] investigated the influence of roasting temperature (300–900 °C) and leaching temperature (20–90 °C) on lithium extraction with 15% H_2SO_4 from coal residue. They confirmed that lithium leaching efficiency increased with calcination temperature, reaching a peak of 99.6% at 500 °C, while higher calcination temperatures decreased lithium extraction (20% at 900 °C). This behavior was attributed to the combustion of carbon and part of the kaolinite (300–400 °C), the complete disappearance of kaolinite (500 °C), followed by the formation of a new phase (trolleite), which renders lithium into a structural element unable to dissolve in sulfuric acid. The effect of acid concentration (0%–30%) and leaching temperature was also investigated for the material roasted at the optimal temperature. Both factors enhanced lithium dissolution, with 15% H_2SO_4 at 90 °C identified as the best condition (further increase in acid concentration did not affect lithium extraction). The lithium extraction from the roasted coal gangue also depended on the process duration (up to 1 h), reaching stable levels close to 100% after 40 min under optimal acid concentration and leaching temperature. Kinetic modeling (shrinking core model) of the leaching process showed that lithium extraction was controlled by diffusion through a solid film of aluminosilicate minerals, which still existed after acid leaching.

A roasting activation–sulfuric acid leaching procedure was further utilized by Kang et al. [100]. They established that lithium leaching efficiency is dependent on the roasting temperature, with the optimal conditions being 650 °C for 1 h, achieving 73% lithium extraction in 5 M H_2SO_4 at 110 °C. This effect was attributed not only to the phase transformation of kaolinite but also to the complete combustion of organic matter, reduction in the size of coal gangue particles, and increase in pore dimensions, leading to a larger surface area available for reaction with the leaching agent. The authors also studied lithium extraction under various leaching conditions, including leaching temperature (70–130 °C), acid concentration (3–7 M), solid-to-liquid ratio (1:3–1:20), and leaching time (0.5–2.5 h).

Unconventional leaching was proposed by Shao et al. [94]. After thermal activation (400–800 °C, 0.5–3 h) of coal gangue, nitric acid was used as the leaching agent (90–170 °C, 0.5–2.5 h, autoclave). Although HNO_3 is rarely used due to its high cost, the authors highlighted its oxidizing properties, which result in iron gathering in the solid phase as hematite. They also pointed out the low cost of acid regeneration and the low decomposition temperature of $Al(NO_3)_3 \cdot 9H_2O$ for alumina recovery as additional advantages. The study found that kaolinite completely converts to metakaolinite in coal gangue in just 0.5 h at 550 °C during thermal activation. This was followed by leaching using HNO_3 dosages calculated according to the molar ratio of acid to total metals (Al, Fe, Ca, Mg, K, and Na) in the material. It was observed that lithium leaching was practically independent of activation temperature and only slightly decreased with activation time. Similarly, the leaching temperature, HNO_3 dosage, liquid-to-solid ratio, and leaching time did not significantly affect lithium extraction, which remained at the levels of 80 ± 5%. Interestingly,

only 2% of iron dissolved into the solution, demonstrating good separation of this impurity during leaching.

Inorganic acids are conventional and quite effective leaching agents, but they are very aggressive on equipment and can pose serious environmental issues, and excess acid needs to be neutralized before the subsequent purification process. Alternatively, organic acids can be used during the leaching stage. Although they are relatively expensive, their undeniable advantages include environmental friendliness, biodegradability, and recyclability. These compounds can dissolve inorganic components not only through the action of hydrogen ions but also enhance leaching due to their complexing properties, forming stable chelates with metal ions.

Xie et al. [98] proposed a novel strategy for scalable lithium leaching from coal-based lithium ore using a reusable organic acid. The calcined (500 °C) raw material was subjected to leaching in water and oxalic acid solutions (2–12 M) at higher temperatures (70–90 °C) due to the poor solubility of the acid in water at low temperatures. This process was carried out at various times (10–180 min) and using different solid-to-liquid ratios (1:3–1:10). Leaching of the calcined material in water resulted in low lithium extraction (8%–12%), mainly from decomposed organic matter. Increasing both the temperature and acid concentration enhanced lithium leachability (up to 90%) due to the increased concentration of H^+ ions in the solution and their accelerated movement to the solid as the process was chemically controlled. Excess oxalic acid in the leaching solution can be recovered by recrystallization at low temperatures (in a refrigerator), but over 90% acid recovery can be achieved only from more concentrated spent solutions (8–12 M); no successful acid recovery can be performed from 2 M $H_2C_2O_4$. The lithium leaching efficiency and recovery rate of oxalic acid remained stable (both about 89%) until the fourth cycle, after which acid recovery decreased while the lithium leaching rate was maintained.

Chen et al. [101] performed thermal activation of coal gangue at different temperatures (300–700 °C, 0.5 h) in static air, air, and nitrogen atmospheres. This was followed by leaching with 0.2 M $(NH_4)_2SO_4$ at pH 4 (60 °C, 3 h), as NH_4^+ ions were considered to have a higher exchange capacity than H^+ ions, thus potentially improving the replacement of Li^+ from clay minerals. The leaching results were poor, with the best lithium extraction of about 10% for the material thermally activated under a nitrogen atmosphere at 400 °C. The results improved somewhat when more acidic leaching solutions were used, resulting in about 45% lithium extraction at pH 1. Sequential analysis of the thermally activated samples indicated a transformation of lithium states from residual (i.e., bonded to clay minerals) mainly to oxide or organic states.

Qin et al. [95] conducted experiments on roasting coal gangue with different ammonium salts (chloride and/or sulfate) at 200–400 °C (1 h), followed by leaching with deionized water (60 °C, 1 h). Lithium dissolution was low (up to 3%), but it increased to 37%–65% when the coal gangue was roasted with $(NH_4)_2SO_4$ at temperatures of 300–400 °C. The results were further improved to nearly 81% by roasting the coal gangue with a mixture of chloride and sulfate ammonium salts at 400 °C, followed by water leaching. The authors concluded that combined roasting with a mixture of ammonium salts strongly promotes the dissolution of lithium, as well as aluminum, through the decomposition of $(NH_4)_2SO_4$ to NH_4HSO_4. NH_4HSO_4 reacted with kaolinite to form $NH_4Al(SO_4)_2$, increasing the specific surface area available for subsequent leaching. Additionally, HCl produced by the decomposition of NH_4Cl promoted further dissolution of the micropores, as indicated by a significant increase in the specific surface area of the final water-leached gangue (from 16 m^2/g to 222 m^2/g). The application of ammonium salt roasting avoided the need for acid consumption during leaching, prevented silica dissolution during water leaching, and was environmentally friendly and energy efficient.

Baking is a roasting method performed at relatively low temperatures, making it a low energy-consuming alternative compared to calcination or traditional roasting. Xie et al. [99] conducted acid baking followed by water leaching. The coal gangue was baked with concentrated H_2SO_4 (40%–98%) at various temperatures (150–200 °C) and different baking

times (20–120 min). During baking, the lithium-bearing kaolinite (98.9% Li) was partially converted into water-soluble aluminum sulfate and partially into insoluble pyrophyllite and boehmite. This conversion facilitated the release of lithium into the solution during subsequent leaching. It was observed that under optimal baking conditions (as detailed in Table 5), the leaching temperature (20–100 °C) and time (ranging from 40–120 min) did not significantly affect lithium extraction, which reached 84%. This indicates that effective lithium recovery can be achieved at room temperature within a relatively short time of 40 min.

Kaolinite in coal gangue belongs to the phyllosilicate minerals, known as 'sheet silicates'. These minerals can be modified by intercalation pretreatment at temperatures below 100 °C. This method does not destroy the layered structure of the mineral but expands its interlayer spacing, thereby saving energy compared to the calcination method. Chen et al. [28] used dimethyl sulfoxide DMSO (DMSO: H_2O 9:1, 60 °C, 24 h, stirring) for intercalation. The solid sample was then leached with 3 M HCl (90 °C, 3 h), resulting in an improvement in lithium extraction to approximately 17.6%. This increase in extraction efficiency was attributed to the presence of lithium on the kaolinite surface through lattice substitution and primarily to the increase in interlayer spacing of some kaolinite from 0.72 nm to 1.10 nm caused by DMSO, without destroying the lattice structure. This enlargement of the reaction area of kaolinite enabled easier entry of hydrogen ions into the [001] interlayer of the mineral. Interestingly, X-ray diffraction of the solid residue showed that DMSO was removed from the interlayers during acid leaching, and the layer spacing returned to its original state, while kaolinite retained its original structure. Simultaneously, calcite, initially present in the coal gangue, was dissolved by the acid, as indicated by the disappearing diffraction peaks.

In another study, Chen et al. [101] conducted comparative investigations on the effect of intercalation by DMSO (60 °C, 24 h, S/L 1:10) and 1 M CH_3COOK (70 °C, 24 h, S/L 1:10) on lithium leaching using 0.2 M $(NH_4)_2SO_4$ at pH 4.0 (60 °C, S/L 1:30, 3 h, 500 rpm). They observed lithium extraction rates of approximately 0.3% from raw coal gangue, 5% from material intercalated with DMSO, and 0.1% from material intercalated with CH_3COOK. The study indicated that DMSO, as an organic polar solvent, can dissolve lithium from organic matter as well as portions of carbonate and Fe–Mn oxide fractions. Simultaneously, the expansion in interlayer spacing facilitated the entry of H^+ and NH_4^+ ions into the [001] interlayer of kaolinite, thereby increasing the reaction area. It was speculated that this portion of lithium ions existed within the kaolinite lattice via ionic bonds rather than belonging to the ion-exchangeable state of the interlayer.

Qin et al. [96] proposed a multistep pretreatment of coal gangue involving intercalation with CH_3COOK, delamination in water under ultrasonication, drying, and roasting with $(NH_4)_2SO_4$. The intercalation process increased the spacing between kaolinite layers from 0.7 nm to 1.3 nm, indicating the introduction of potassium acetate into the mineral interlayer. TEM observations revealed a lamellar curl phenomenon on the particle surface, achieved by eliminating interlayer hydrogen bonds and atomic interactions. Intercalation and delamination resulted in a reduced number of kaolinite layers and particle size, as well as an increased specific surface area for the reaction.

The material was further roasted to induce compositional changes according to the following reactions:

$$(NH_4)_2SO_{4\,s} \rightarrow NH_4HSO_{4\,l} + NH_{3\,g} \quad (6)$$

$$NH_4HSO_{4\,l} + Al_2Si_2O_5(OH)_{4\,s} \rightarrow 2NH_4Al(SO_4)_{2\,s} + 2NH_{3\,g} + 5H_2O_{\,g} + 2SiO_{2\,s} \quad (7)$$

The roasting product was then leached with water (in the same vessel). It was found that the delamination pretreatment increased the lithium leaching rate from 72% to 86.6%, compared to solely roasted material. Speciation studies of the raw coal gangue and the roasted product (using the Tessier method) revealed changes in the lithium occurrence mode. While almost all lithium in the raw gangue was residual, roasting transformed 75% of lithium into an exchangeable form. Interestingly, other metals that existed in the residual

state in the coal gangue also transformed into an exchangeable form during roasting, except for As and Cd.

It is worth noting that the proposed process can fully recover ammonia and ammonia-containing wastewater, reducing the cost of reagents crucial for roasting. Gradual lithium enrichment in the cyclic ammonium salt was also observed, but after several cycles, this enrichment slowed lithium extraction from the raw material due to limitations from the dissolution balance. Lithium was recovered from the cycled ammonium salt as carbonate by precipitation with $(NH_4)_2CO_3$.

Chen et al. [101] developed a two-step pretreatment procedure involving grinding and thermal activation (400 °C, nitrogen atmosphere), followed by leaching with $(NH_4)_2SO_4$ solutions of varying pH (1.0 and 4.0). They observed enhanced lithium dissolution and inhibited aluminum dissolution, particularly at a pH of 4.0. Extending the grinding time (10–90 min) positively affected lithium extraction, especially at pH 1.0, where an extraction level of 84% was stabilized after 1 h of grinding. The grinding treatment deformed or even destroyed the octahedron in the kaolinite crystal structure, exposing more Li^+ to the lattice surface. These lithium ions could migrate out of the octahedron, making them easier to leach. Grinding and thermal activation altered the mode of lithium occurrence. In the pre-treated material, lithium was found mainly in oxide and organic matter fractions, with only 17% of lithium remaining in the residual state. In comparison, about 96% of lithium was in the residual state in the raw coal gangue.

Extracting lithium ions from coal gangue into the leaching solution is accompanied by the transfer of other metal ions present in the feed material. These cations, including aluminum, magnesium, calcium, titanium, iron, and lead ions, exist in varying concentrations. Therefore, developing methods for the selective recovery of lithium from leach liquor is essential, yet this issue has not been practically addressed. Some research studies have explored lithium recovery from various solutions using precipitation, solvent extraction, ion exchange, membrane technologies, or adsorption processes [107–109]. However, these methods have not been examined in the context of components derived from coal gangue leaching. It is important to consider that coal gangue contains other valuable metals, necessitating a comprehensive approach for the effective utilization of both the raw material and the leachate.

4.5. Lithium Separation

The sole study on lithium recovery from coal gangue leachate was conducted by Long et al. [110]. They synthesized a $Li_{1.6}Mn_{1.6}O_4$ precursor using a two-step method involving microwave-assisted hydrothermal synthesis and solid-phase calcination. Acid pickling of the precursor produced the ion-sieve $H_{1.6}Mn_{1.6}O_4$ (HMO), which exhibited a Li^+ adsorption capacity of approximately 29 mg/g. The adsorption properties were investigated using, among other solutions, what was obtained after acid leaching of calcined coal gangue [97]. The acidic chloride leachate contained approximately 48 mg/L Li^+, along with Na^+, Mg^{2+}, Al^{3+}, and Ca^{2+} at unspecified concentrations. Given that HMO demonstrated enhanced lithium uptake in an alkaline environment, the pH of the leach liquor was increased to 13. This adjustment led to the formation of colloidal metal hydroxide particles that adsorbed some of the lithium ions, thereby reducing the overall lithium content in the solution. Despite this, HMO exhibited an adsorption capacity of approximately 5 mg/g for Li^+ and lower capacities for accompanying metal cations (0–0.8 mg/g). It resulted in 99.9% lithium recovery. The high selectivity of HMO for lithium ions was attributed to the ion-sieve effect, which originates from the unique three-dimensional tunnel structure within the lattice that prevents the adsorption of larger ions due to greater steric hindrance.

5. Recovery of Lithium from Coal Fly Ash

5.1. Coal Fly Ash

Combustion of coal in coal-fired power plants generates various waste products, commonly referred to as 'coal ash' [111]. This category includes several by-products such

as fly ash, bottom ash, boiler slag, and flue gas desulfurization material. Among these, coal fly ash constitutes the majority, representing about 40%–90% of the total combustion residue [112,113].

Fly ash is a very fine (10–200 μm), powdery material, ranging in color from dark brown to light gray (Figure 7). This industrial waste residue is formed from organic matter, clay, and associated minerals after the high-temperature combustion (1300–1700 °C) and cooling of coal in coal-fired power plants. The particles of fly ash are typically captured from flue gas and collected by electrostatic or mechanical precipitation. It is estimated [114] that for every four tons of coal burned, one ton of fly ash is generated. This corresponds to approximately 600–800 million tons of coal fly ash produced annually worldwide [115]. Although coal fly ash can be beneficially reused in products such as concrete, geotechnical materials, zeolite, or soil amelioration [116–119], its global utilization rate is estimated at 25%–64% of the total production [112,119,120]. Consequently, a large percentage of fly ash is stored in landfills and ash ponds (surface impoundments). The disposal of these massive quantities of fly ash is a significant environmental concern, as the particles can travel up to 40–50 km with the wind, spreading over an area of up to 150,000 km^2. This can lead to land degradation, severe air, and water pollution, and health problems for plants, animals, and humans due to a risk of dissolution of toxic heavy metals (e.g., chromium, arsenic, cadmium, and lead) from the ash [112,115,121].

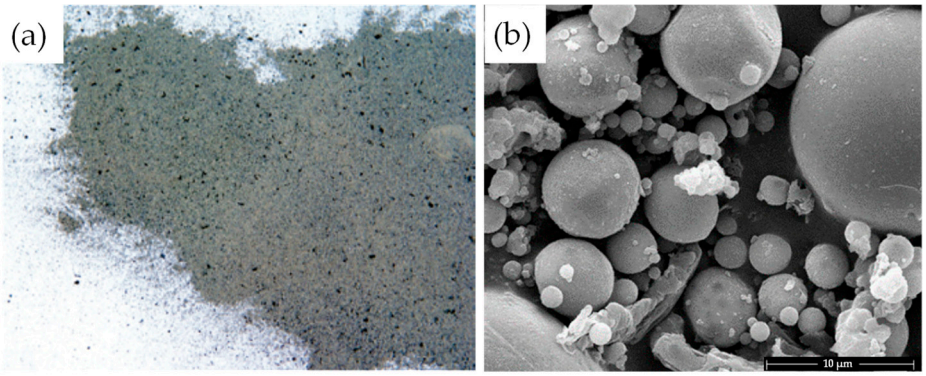


Figure 7. Coal fly ash: (**a**) macroscopic view (black particles of unburned coal) [122], (**b**) SEM micrograph [123].

Coal fly ash is primarily composed of silicates, oxidized metals, and carbonaceous combustion fragments. Depending on the type of coal, the fly ash can contain 13%–60% SiO_2, 5%–35% Al_2O_3, 4%–40% Fe_2O_3, 1%–40% CaO, as well as MgO, Na_2O, and K_2O, each below 10%. Amorphous glass represents the main mineralogical component of the coal fly ash (over 50%), but quartz (silicates), mullite (aluminosilicates), magnetite and hematite (iron compounds), calcite and dolomite (carbonates), anhydrite (sulfate), and other minerals are also present [122–147]. Laboratory investigations [147] revealed that the phase composition of fly ash changes sequentially with increasing coal combustion temperature. Kaolinite, boehmite, and calcite were found to be the main components at 400 °C, while the crystalline phases became more abundant and transformed into mullite, corundum, and plagioclase as the combustion temperature reached 1300 °C. The proportion of unburned carbonaceous residues (usually in the glass phase) in fly ash can range from about 1% to 20%, depending on the combustion efficiency.

The particles of fly ash are enriched in some elements, mainly those that are volatile and can partially condense in the flue gases of the combustion system. These elements include As, B, Bi, Cd, Ge, Ga, Hg, Ti, and others. Through the combustion process, the concentration of trace elements in fly ash can be enriched up to several dozen times, depending on the feed coal.

Gong et al. [146] proposed a law governing the formation of fly ash during coal combustion. In coal, inorganic components like kaolinite and boehmite are associated with

organic carbon. During combustion, carbon is oxidized to carbon dioxide, while aluminum and silicon recombine to form mullite, corundum, and glass. Mullite and corundum form finer particles, while the glass phase binds other materials to create larger particles. This process results in the enrichment of metals in the smaller-sized particles of the fly ash.

5.2. Occurrence Modes of Lithium

Coal ash also contains valuable elements, including lithium. During combustion, lithium is significantly concentrated in the fine particles of fly ash (Table 6), resulting in higher concentrations than in the original coal and much higher than in bottom ash [104,130]. For example, Pougnet et al. [54] investigated the lithium content in about one hundred samples of coal and coal fly ash collected from eleven major South African power stations. They reported that lithium levels in coal ranged from 45 ppm to 81 ppm, while the results for the corresponding ashes ranged from 77 ppm to 359 ppm, indicating that fly ash contained 1.5 to 5.2 times more lithium than coal. Similar levels of lithium enrichment in coal fly ashes have been reported by other authors [104,130–134].

Table 6. Lithium occurrence in coal fly ashes.

Source	Content, ppm	Lithium Host Phase	Ref.
Pingshuo Coal Gangue Power Plant, China	190	Uncertain	[104]
	470	No data	[143]
Power plants, China		Glass, aluminosilicate, magnetic	[129]
Gouha Jungar, Inner Mongolia	412		
Datang Togtoh, Inner Mongolia	375		
Datong, Shanxi	266		
Yangquan, Shanxi	267		
Jungar Power Plant, China	453 *	Glass	[130]
Chongqing Power Plant, China	197	Aluminosilicate glass, mullite, quartz	[131]
Tashan Power Plant, China	196	Glass	[132]
Pingwei Power Plant, China	57	Aluminosilicate, glass	[134,140]
Shuozhou Thermal Power Plant, China	930 **	Lithium silicate, glass	[135]
Thermoelectric Power Plant, China	403	No data	[136]
IMDIRRD Co., Ltd., Honhot, China	632 ***	No data	[139]
Power plant, China	502	Aluminosilicate glass	[142]
Pulverized coal-fired power plants, Europe		No data	[127]
Monfalcone, Italy	161		
Sardegna, Italy	377		
Barrios, Spain	311		
Espiel, Spain	303		
Teruel, Spain	256		
Hemweg-8, The Netherlands	329		
Thermal power plants, Greece		Amorphous glass	[128]
Ag. Demetrios	95–126		
Achlada	256		
Megalopolis	211		
Aminteon	155		
Coal power plant, Iran	648	No data	[137,138]
Coal-fired power plant, Coahuila, Mexico	99	No data	[126]
Power stations, South Africa		No data	[54]
Komati	160–207		
Duvha	182–270		
Matla	228–359		

* 413 ppm in wet coal fly ash; ** recalculated from 0.2% Li_2O; *** recalculated from 1145.16 μg/g Li_2O.

Ma et al. [104] stated that, unlike coal and coal gangue, no strict mode of lithium occurrence in the fly ash could be identified, as the inorganic matter underwent a series of complex reactions during coal combustion, leading to a scattered distribution of the

element. Moreover, no definitive trend in the variation of lithium was observed in particles of different sizes.

Pentari et al. [128] identified the prevailing form and association of lithium in coal fly ashes from thermal power plants in five different areas of Greece. They did not detect any lithium-bearing phases in the materials but found a strong positive correlation between aluminum content and amorphous material, concluding that lithium is likely hosted in the amorphous glassy phase. Sequential extraction experiments, performed using the Tessier and BCR methods, revealed that most of the lithium (69%–89%) was strongly bound to the mineral matrix and not in readily releasable forms.

Hu et al. [129] investigated high-alumina coal fly ashes derived from several Chinese power plants. They confirmed a positive correlation of lithium with aluminum and silicon. Most of the lithium (79%–94%) was found in the glass fraction, with only 5%–16% in the mullite–corundum–quartz phase and less than 5% in magnetic particles (iron oxide). However, more detailed investigations ruled out quartz as a lithium carrier, while lithium is significantly enriched in glass under different coordination structures.

Dai et al. [130] compared dry and wet high-alumina coal fly ashes. They found somewhat less lithium in wet ash (413 ppm) with larger particle sizes (67–92 μm) compared to dry material (453 ppm; 35–66 μm). The distribution of lithium in fractions of different particle sizes (25–120 μm) of dry fly ash was relatively uniform, with enrichment factors around 0.8–0.9. Distinct lithium dispersion was observed in the mineral fractions: glass (682 ppm), mullite–corundum–quartz (76 ppm), and magnetic phases (31 ppm), which represented 55%, 43%, and 2% of the total ash mass, respectively.

A detailed analysis of lithium occurrence in different phases and fractions of Chinese coal fly ash (197 ppm Li) was conducted by Xu et al. [131]. They divided the ash into five particle size fractions (from <25 μm to >75 μm) and found that, in general, lithium content increased as particle size decreased, with the highest concentration (218 ppm) in particles of 25–38 μm, which represented only 19% of the total ash mass. The ash was also separated into magnetic and non-magnetic fractions, with the latter accumulating 60% of the total lithium. This was then correlated with lithium accumulation in aluminosilicate glass. The sequential extraction procedure (Figure 8) revealed that about 57% of the lithium was glass-bound, while almost 30% was present in mullite and quartz. The remaining lithium was distributed mainly among organic/sulfide, metal-oxide, and ion-exchangeable forms.

Other studies [132,146] further confirmed lithium enrichment in fine-grained fractions of the fly ash, which is an opposite trend compared to lithium concentration in particle fractions of coal gangue. Shao et al. [132] reported 230–240 ppm Li in particles with dimensions below 57 μm in high-alumina coal fly ash (196 ppm Li). Although all size fractions had a similar mineralogical composition, it was found that as ash particles became finer, the content of corundum, quartz, and glass increased, while mullite decreased. The authors pointed out that while high-lithium fractions of the ash have extraction potential, the high content of harmful elements, such as cadmium, requires special attention due to its high enrichment factor in the ash fractions.

Numerous studies [104,130,132,133] have shown that lithium is primarily enriched in fly ash after coal combustion, predominantly in a glass phase. Xu et al. [133] discussed changes in lithium occurrence modes in coal combustion products under different conditions, such as combustion temperature (400–1000 °C) and atmosphere (O_2/CO_2 or O_2/N_2), emphasizing that the volatilization rate of lithium depends on these factors. During combustion, minerals and organic matter in coal undergo various complex reactions (i.e., carbonization, dehydration, dehydroxylation, decomposition, oxidation, volatilization, and crystallization. These complex processes affected the phase changes and distribution of lithium in coal fly ash (Figure 9). In feed coal, lithium exists predominantly in octahedral sites of kaolinite and illite/smectite, but at high-temperature combustion, the porosity of clay minerals increased due to dehydration and dehydroxylation of kaolinite and illite/smectite. This process is accompanied by the formation of highly active amorphous phases, which enable lithium activation, especially at a combustion temperature of 500 °C.

At temperatures higher than 500 °C, the amorphous phases begin to aggregate and recrystallize into pseudomullite and mullite, decreasing the proportion of easily leachable lithium (Figure 9b). Notably, in oxy-fuel combustion (O_2/CO_2), the amount of easily leachable lithium was relatively higher compared to air combustion (O_2/N_2).

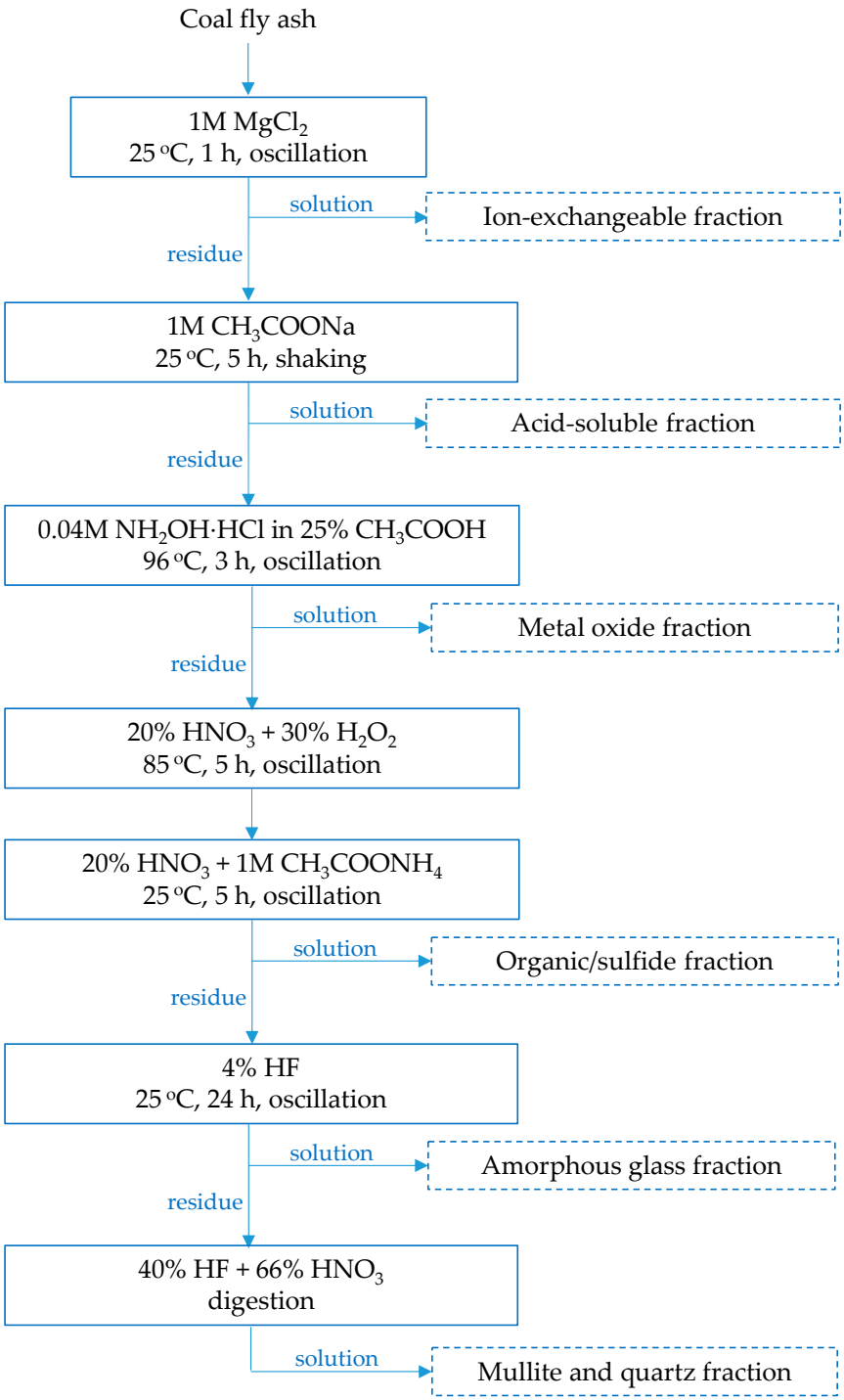


Figure 8. Scheme of sequential chemical extraction of lithium from coal fly ash [131].

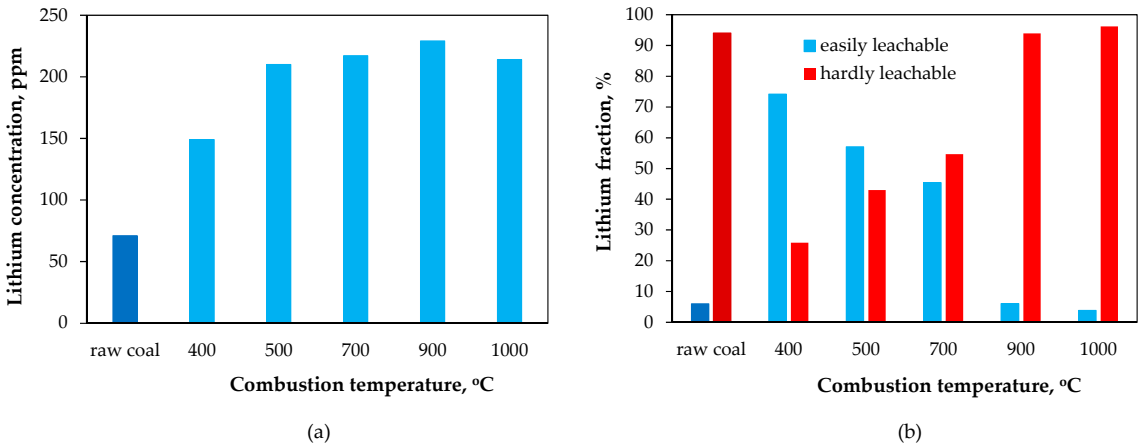


Figure 9. Influence of combustion temperature on lithium concentration in coal ash (**a**) and its leachability from coal fly ash (**b**) [133].

Although Xu et al. [133] investigated the modes of lithium occurrence in fly ashes generated during coal combustion at different temperatures, the specific lithium-host phases remained unclear. However, theoretical simulations indicated that the most probable mineral forms include lithium aluminosilicates ($LiAlSiO_4$, $LiAlSi_2O_6$, $LiAlSi_4O_{10}$), lithium manganese oxide ($LiMn_2O_4$), lithium iron oxide ($LiFeO_2$), and lithium sulfate (Li_2SO_4). It should be noted that Li et al. [135] detected lithium silicate (0.9%) in coal fly ash during phase analysis.

Taking into account experimental and theoretical considerations, Xu et al. [133] proposed a mechanism for lithium hosting during coal combustion. Initially, after calcination at 400 °C, most of the lithium is released from the octahedral sites of kaolinite and illite/smectite in coal. This release enables lithium to react with Fe, Mn, and S, forming lithium manganese/iron oxides and lithium sulfate, respectively, which changes the lithium from a hardly leachable form to an easily leachable form (Figure 9b). As the temperature increases further (500–1000 °C), lithium ions migrate back to the octahedral positions of clay minerals to form lithium aluminosilicates or become non-leachable due to the densification of aluminosilicate glass.

5.3. Lithium Pre-Enrichment Methods

Based on lithium's tendency to spread among phases of different particle sizes, densities, or magnetic properties, Li et al. [134] recommended a combination of physical separation methods to effectively enrich the element from coal fly ash of relatively low lithium concentration (about 57 ppm). Previous studies [130–133,146] showed that lithium tends to accumulate in the residual form of aluminosilicates and glass (90%), in non-magnetic material (66 ppm), in particles smaller than 45 µm (68 ppm), and in light density fractions of 1.8–2.0 g/cm^3 and below (about 70 ppm). Thus, a concept of separation procedures (Figure 10) was proposed to achieve efficient lithium enrichment before further hydrometallurgical recovery. It involved particle sieving followed by magnetic separation to obtain a non-magnetic fraction enriched in lithium, which is then directed to the leaching stage.

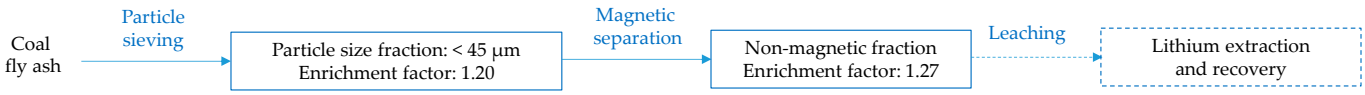


Figure 10. Scheme of sequential physical enrichment of lithium in coal fly ash [134].

5.4. Lithium Extraction

The existence of barely soluble lithium-hosting phases (aluminosilicate glass) in the coal fly ash requires special treatment to disrupt silicon–oxygen–aluminum bonds and

release lithium during leaching. Most of the research studies [113,116–119,145,146] focused on aluminum recovery from coal fly ash due to its high concentration in the material. From there, the experience gained facilitated the development of processing methods for the recovery of other valuable metals [124,131,144]. Nevertheless, research aimed at recovering lithium is still quite limited, having only begun in the last few years (Table 7).

Table 7. Optimal conditions of lithium recovery from coal fly ash CFA (lithium concentration in the feedstock is shown in Table 6, according to the references).

Pretreatment Stage	Leaching Conditions	Lithium Extraction	Ref.
One-step pretreatment			
Pre-desilication 0.4 M NaOH, 120 °C, S/L 1:3, 1 h, 300 rpm	6 M HCl, 120 °C, S/L 1:20, 4 h	82.2%	[135]
Salt activation NH4F (SiO_2/NH_4F 1:1.35), 155 °C, 2 h	H_2O, 70 °C, S/L 1:10, 2 h	90.8%	[136]
Roasting Na_2CO_3 (CFA/Na_2CO_3 1:0.5), 850 °C, 2 h	0.5 M HCit, 30 °C, 1 h, 450 rpm	97.3%	[137]
Na_2CO_3 (CFA/Na_2CO_3 1:0.5), 850 °C, 2 h	Ps. putida, 75 °C, S/L 3:100, 500 rpm	97.0%	[138]
Na_2CO_3 (CFA/Na_2CO_3 1:1), 875 °C, 1.5 h	0.4 M HCit, 50 °C, 1 h, S/L 1:125, 400 rpm	90.5%	[141]
Na_2CO_3 (CFA/Na_2CO_3 1:1), 800 °C, 2 h	3 M HCl, 90 °C, S/L 1:20, 3 h	90.4%	[142]
Mechanical activation ball mill (CFA/ball 1:3.5), 1 h, 500 rpm	5 M NaOH, 95 °C, S/L 1:20, 2 h	91.6%	[139]
Multi-step pretreatment			
I. Calcination 800 °C, 3 h II. Mechanochemical activation $Na_2S_2O_7$ (Al_2O_3/$Na_2S_2O_7$ 1:8), 1 h, 300 rpm	$Na_2S_2O_8$ (Al_2O_3/$Na_2S_2O_8$ 1:3), H_2O, 200 °C, 2.6 MPa, S/L 1:4, 2 h, 300 rpm	71.6%	[140]
No pretreatment			
	20% HCl, 95 °C, S/L 1:5, 2 h	92.7%	[147]
	3.9 M NaOH, 95 °C, S/L 1:5, 2 h	42.0%	
	alternate multistep leaching: acid–alkali–acid–alkali–acid: 6.3 M HCl, 5 M NaOH, 90 °C S/L 1:5, 2 h, stirring	84.0%	[143]
	pressure leaching: 40% H_2SO_4, 140 °C, S/L 1:3, 2 h (lab-scale)	94.2%	[144]
	53% H_2SO_4, 160 °C, S/L 1:3, 2 h (pilot-scale)	88.9%	

The transformation of insoluble aluminosilicate glass into easily soluble sodium salt is the most common method of fly ash pretreatment. This can be achieved using NaOH solutions [129,135] or through alkaline fusion [137,138,141,142].

Sodium hydroxide is a chemical reagent that readily reacts with alumina and silicate-type minerals. Li et al. [135] showed that during pre-desilication, silica SiO_2, mullite $3Al_2O_3{\cdot}2SiO_2$, and corundum Al_2O_3 were removed (totally or partially) from the coal fly ash, while hydroxy sodalite $Na_8(AlSiO_4)_6(OH)_2{\cdot}2H_2O$ was generated in a solid form. Thus, the following reactions could occur during interaction with the alkali solution:

$$SiO_{2\,s} + 2NaOH \rightarrow Na_2SiO_3 + H_2O \quad (8)$$

$$Al_2O_{3\,s} + 2NaOH + 3H_2O \rightarrow 2Na[Al(OH)_4] \quad (9)$$

$$3Al_2O_3{\cdot}2SiO_{2\,s} + 8NaOH \rightarrow Na_8(AlSiO_4)_6(OH)_2{\cdot}2H_2O_{\,s} + H_2O \quad (10)$$

$$6Na_2SiO_3 + 6Na[Al(OH)_4] \rightarrow Na_8(AlSiO_4)_6(OH)_2{\cdot}2H_2O_{\,s} + 10NaOH + 4H_2O \quad (11)$$

Gong et al. [146] stated that during desilication, the main reaction (8) is accompanied by the formation of fine sodalite particles:

$$10Na_2SiO_3 + 3Al_2O_3 + 19H_2O \rightarrow Na_6Al_6Si_{10}O_{32} + 14NaOH \quad (12)$$

Large amounts of these particles can adhere to the surface of mullite, decreasing the desilication efficiency. It was estimated that such a zeolite phase accounted for about 23% of the total mass of the desilicated ash.

The desilicated coal fly ash was pre-leached with 6 M acids: HCl, HNO_3, H_2SO_4, HF (120 °C, S/L 1:20, 4 h, in an incubated sealed hydrothermal reaction kettle), resulting in lithium extractions of 78%, 72%, 75%, and 79%, respectively [135]. Due to the highest simultaneous aluminum leachability, HCl was selected as the most suitable solvent. Further optimization of the leaching conditions (acid concentration, temperature, S/L ratio, process duration) revealed that the best lithium dissolution (about 82%) and optimal acid consumption could be achieved with 6 M HCl. A comparison of lithium recovery from untreated and desilicated coal fly ashes showed a significant increase in leaching efficiency, as illustrated in Figure 11. It was also observed that during the hydrochloric acid pressure leaching process, the spherical particles of desilicated fly ash decomposed into flakes, the mullite phase partially dissolved, and most of the glass phase leached into the liquor. The decreased leaching rate of lithium at the later stages of the process was attributed to the formation of a silicate layer that limited lithium transport from the bulk of the ash particles.

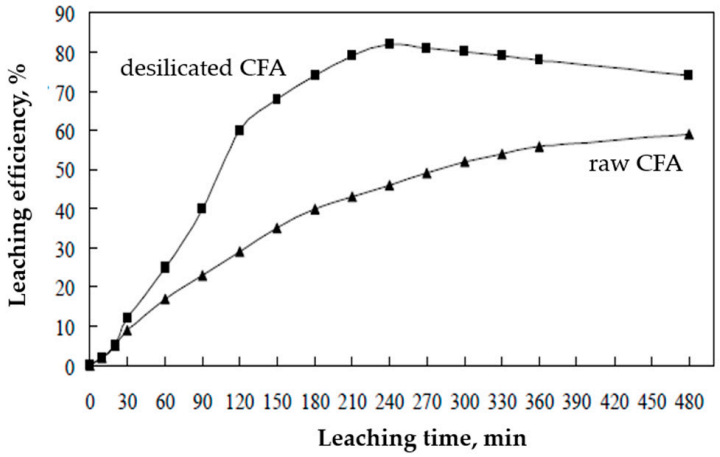


Figure 11. Time-dependent lithium extraction from raw and desilicated coal fly ashes under optimal leaching conditions: 6 M HCl, 120 °C, S/L 1:20 [135].

Hu et al. [129] proposed a general flowsheet for the recovery of lithium (and aluminum) involving desilication with NaOH solution. Although they did not discuss it in detail, they suggested using adsorption separation to extract lithium from the pre-desilication solution.

Alkali fusion, specifically roasting with Na_2CO_3, is the most frequently proposed method for pretreating coal fly ash [137,138,141,142]. During the roasting process, aluminosilicate and silicate minerals (e.g., mullite) convert into sodium aluminosilicate, which is soluble in water and acids [137]:

$$3Al_2O_3{\cdot}2SiO_2 + 4SiO_2 + 3Na_2CO_3 \rightarrow 6NaAlSiO_4 + 3CO_2 \quad (13)$$

Alternatively, NaCl [137,141], $NaNO_3$, Na_2SO_4 [137] as well as NaOH, CaO, and $CaCO_3$ [141] have been examined as roasting additives. However, the resulting products were not as easily leachable as those obtained with sodium carbonate.

Rezaei et al. [137] optimized the lithium recovery process by analyzing the effects of various roasting agents (sodium salts), salt/ash ratios (0.5–2), leaching reagents (acetic, citric, oxalic, and malic organic acids), their concentrations (0.25–1.0 M), and leaching times

(1–4 h). The screening tests identified the following order of parameters with the strongest effect on lithium recovery: leaching reagents (56.7%), roasting reagents (22.8%), leaching time (9.2%), solid/salt ratio (6.3%), and acid concentration (5%). The optimal procedure involved roasting with carbonate salt at 850 °C, followed by leaching with citric acid at a relatively low temperature of 30 °C. Under these conditions, about 97% of lithium was dissolved from the solid phase. Kinetic modeling of the leaching process revealed that dissolution is governed by interfacial transfer and diffusion through the product layer, which is composed mainly of silicon and oxygen atoms.

Li et al. [141] employed a similar two-stage lithium recovery process involving alkali fusion with sodium carbonate followed by leaching with citric acid. Under optimal conditions, more than 90% of lithium was extracted into the solution. The addition of various ammonium salts (acetate, chloride, sulfate) to the citric acid solution or the use of other organic acids (tartaric, lactic) did not improve the leachability of the roasted product. They also investigated the influence of roasting temperature and time on leaching efficiency, demonstrating that 94 ± 1% of lithium could be recovered at a roasting temperature of 875 °C in just 15 min. Consistent with other studies, the kinetic analysis of the leaching process followed the shrinking core model, indicating that the process was controlled by both internal diffusion and chemical reaction, with the main leaching residue being amorphous silicon.

The chemical leaching of alkali roasting products with organic acids was then compared to leaching using biogenic carboxylic acids. Rezaei et al. [138] investigated the bioleaching process using *Pseudomonas putida* and *Pseudomonas koreensis* as microorganisms that produce organic acids. It was found that both bacterial species primarily generate gluconic acid, with smaller amounts of citric and oxalic acids. The bioleaching experiments showed higher process efficiency in the *Ps. putida* culture medium at 75 °C, resulting in 98% lithium extraction. Interestingly, there was about 25% lower recovery in chemical leaching using commercial organic acids at the same concentration as in the bioleaching system. This suggests the potential role of additional unknown metabolites produced by bacteria, which warrants further investigation.

It is worth noting that the extraction of lithium from coal fly ash roasted with sodium carbonate using organic acids can be more effective than using an HCl solution. Gao et al. [142] reported that 90.4% of lithium was extracted using 3 M HCl, but the extraction rate was 10% higher when using 0.5–2 M citric acid solutions. They proposed a two-step continuous leaching process, using 1 M HCl in the first stage and 2 M HCl in the second. This method allowed for the recovery of 71% of lithium in the first stage, selectively separating it from gallium, which was mainly leached in the more concentrated acid solution. They also observed that the selective separation and leaching of lithium and gallium were influenced by the formation of silicic acid gel during the leaching process at lower acid concentrations.

Thermochemical activation of coal fly ash can also be achieved at lower treatment temperatures, although it requires more aggressive chemical reagents. Xu et al. [136] used ammonium fluoride to transform aluminosilicate glass particles into more soluble forms. This transformation was confirmed by the phase analysis of the products activated at different temperatures:

$$3Al_2O_3 \cdot 2SiO_2 + 12NH_4F \rightarrow 2(NH_4)_2SiF_6 + 8NH_3 + 3Al_2O_3 + 2H_2O \quad (14)$$

$$Al_2O_3 + 6NH_4F \rightarrow 2AlF_3 + 6NH_3 + 3H_2O \quad (15)$$

$$SiO_2 + 6NH_4F \rightarrow (NH_4)_2SiF_6 + 4NH_3 + 2H_2O \quad (16)$$

$$Li_2O + 2NH_4F \rightarrow 2LiF + 2NH_3 + H_2O \quad (17)$$

It was also found that mineral components in the glass phase can react with NH_4F at different temperatures, and the reaction of the glass phase is more thermodynamically favorable than that of the crystalline phase (corundum, mullite). This means that high-

temperature conditions are not required. Consequently, silica and lithium were converted into soluble fluorides, while corundum and mullite remained as undissolved residues during subsequent water leaching. The maximum lithium extraction of 90% was obtained for salt activation temperatures of 155–160 °C.

Xing et al. [139] developed a process for extracting lithium from coal fly ash and separating it from other metals in the aqueous solution. The raw fly ash was first mechanically activated by ball milling with zirconia balls and then subjected to alkaline leaching (2.5–7.5 M NaOH, 55–95 °C, S/L 1:10–1:30, 1–3 h). During leaching, most of the lithium (~93%), which was initially accumulated in the glass phase, migrated to the leaching solution as soluble LiOH. Under optimal conditions, about 92% of lithium could be extracted, and the efficiency was predominantly influenced by leaching temperature and S/L ratio.

A three-step procedure for coal fly ash treatment was proposed by Fang et al. [140]. Initially, after calcination, the inert aluminosilicate glass was activated by milling (in a planetary ball mill) with $Na_2S_2O_7$ additive, converting it into aluminum sodium sulfate and generating $NaHSO_4$ simultaneously:

$$3Al_2O_3{\cdot}2SiO_2 + 9Na_2S_2O_7 \rightarrow 6Na_3Al(SO_4)_3 + 2SiO_2 \quad (18)$$

$$2Na_2S_2O_7 + 2H_2O \rightarrow 4NaHSO_4 \quad (19)$$

During subsequent pressure leaching in the presence of $Na_2S_2O_8$, the following reactions occur:

$$Na_2S_2O_8 + 2H_2O \rightarrow 2NaHSO_4 + H_2O_2 \quad (20)$$

$$2H_2O_2 \rightarrow 2H_2O + O_2 \quad (21)$$

These reactions created conditions that favor the formation of HSO_4^-, which further disintegrates the Al–O–Si bond, releasing lithium cations into the solution:

$$Li_2O + 2NaHSO_4 \rightarrow Li_2SO_4 + Na_2SO_4 + H_2O \quad (22)$$

As a result, lithium extraction efficiency reached about 95%.

Chen et al. [147] compared lithium behavior during acid and alkali leaching of fly ashes produced at different coal combustion temperatures. They found a decrease in leaching efficiency from about 93% to approximately 23% as the combustion temperature increased from 400 °C to 1300 °C and when 20% HCl was used as the leaching agent. High lithium extraction (above 90%) was observed up to 800 °C, followed by a sharp decline for 900 °C and higher combustion temperature. An opposite effect of coal combustion temperature on lithium extraction was observed during leaching in almost 4 M NaOH solution, resulting in the highest lithium recovery of about 42% at 1300 °C. This was attributed to the presence of lithium in amorphous aluminum silicates, which react more readily with acids, and to the reduced lithium volatility at lower coal combustion temperatures, where smaller ash particles were formed.

Direct one-step leaching of raw coal fly ash has proven to be inefficient, especially if fly ashes are generated at higher coal combustion temperatures. However, this can be improved by introducing more complex leaching procedures or using more aggressive leaching conditions. For example, Ma et al. [143] proposed a five-step leaching process using 6.3 M HCl (230 g/L) and 5 M NaOH (200 g/L) solutions at an elevated temperature of 90 °C. This process involved alternating stages of acid–alkali–acid–alkali–acid treatment, with each stage lasting 2 h. The total lithium extraction reached 84%, with 80% dissolved by the HCl solution, predominantly during the first acid treatment (about 45% Li recovery). These variable conditions enhanced the gradual breakdown of Si–O–Al units and the removal of SiO_2, thereby releasing metal ions from the material:

$$Li_2O{\cdot}Al_2O_3{\cdot}SiO_{2\,s} + 8HCl \rightarrow 2LiCl + 2AlCl_3 + SiO_{2\,s} + 4H_2O \quad (23)$$

$$Al_2O_3{\cdot}2SiO_{2\,s} + 6NaOH + H_2O \rightarrow 2Na[Al(OH)_4] + 2Na_2SiO_3 \quad (24)$$

In turn, Li et al. [144] developed an energy-efficient sulfuric acid leaching process that utilizes the heat generated during the dilution of concentrated acid. This process was conducted in an autoclave under self-heating and self-pressure conditions by adding concentrated H_2SO_4 (98%) to the aqueous ash slurry to create solutions of different acid concentrations. In lab-scale experiments, the optimal conditions (140 °C, 40% H_2SO_4) resulted in a lithium leaching efficiency of 94%. The highest lithium extraction in pilot-scale experiments was achieved at 160 °C, controlled by acid dilution to 53%.

5.5. Lithium Separation

Concentrations of lithium in the leachates are low (below 1 g/L), as its content in the leached solid is in the ppm range. Therefore, classical methods [11,15] of separation and recovery of final products are not suitable. Modern technologies, including ionic separation and preconcentration, should be considered for their potential utilization. Techniques such as ion exchange, solvent extraction, membrane technologies, electrodialysis, and adsorption appear to be the most recommended choices. These methods are used for lithium separation from brines [13,25,26,33], but they cannot be directly adopted for lithium recovery from ash leachate due to significant differences in ionic speciation of the solutions. Thus, it is crucial to develop ion exchange methods specifically tailored to these unique electrolytes. The literature shows only a few examples of such specialized techniques (Figure 12). In addition to the solvent extraction from alkaline [139] or acid [148,149] solutions, sporadic modern techniques have been examined like liquid membrane electrodialysis [150], resin adsorption [151], or ion sieve separation [152].

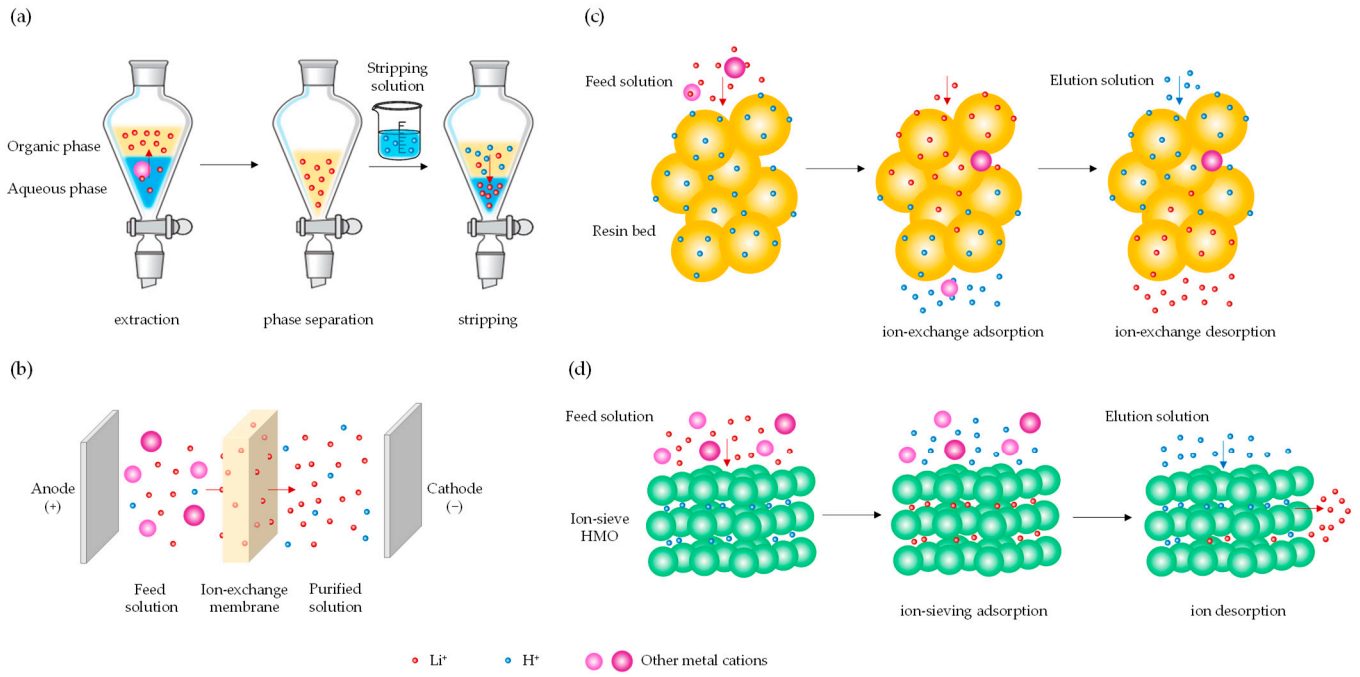


Figure 12. Schemes of lithium-ion separation methods from coal ash fly leachate: (**a**) solvent extraction, (**b**) electrodialysis with ion-exchange membrane, (**c**) ion-exchange with resin, and (**d**) ion-sieving.

Xing et al. [139] selectively recovered lithium from other metal ions (e.g., K^+, Na^+, Zn^{2+}, Al^{3+}, Ga^{3+}, and Fe^{3+}) present in the strong alkaline (NaOH) leachate as simple cations or hydroxo complexes. For this purpose, solvent extraction with a mixture of benzoyltrifluoroacetone HBTA and trioctylphosphine oxide TOPO extractants was used. These extractants exhibit a synergistic effect during lithium extraction under alkaline conditions:

$$OH^- + HBTA \rightarrow BTA^- + H_2O \quad (25)$$

$$nBTA^- + Na^+ + mTOPO \rightarrow Na{\cdot}nBTA{\cdot}mTOPO \quad (26)$$

$$Li^+ + Na{\cdot}nBTA{\cdot}mTOPO \rightarrow Li{\cdot}nBTA{\cdot}mTOPO + Na^+ \quad (27)$$

Lithium concentration in the leachate reached 10 mg/L, while the total concentration of other metal cations was about 5 g/L. Lithium extraction efficiency reached over 99% in three consecutive extraction stages (HBTA/TOPO 1:1, O/A 1:1, 2 min). Lithium ions were then stripped from the organic phase using an aqueous HCl solution (2 M, O/A 20:1). The extraction process demonstrated high selectivity, with the distribution coefficient for lithium reaching 2, while for remaining metal impurities the values were below 0.07.

Rui et al. [148] performed solvent extraction of lithium from a solution obtained during the leaching of high-alumina coal fly ash with HCl. The solution contained only 0.4 g/L Li^+, approximately 93 g/L Al^{3+}, and other cations (Mg^{2+}, Ca^{2+}, Fe^{3+}, K^+, and Na^+) in a total amount of about 10 g/L, as well as around 343 g/L Cl^-. They used a mixture of tributyl phosphate TBP (70 vol%), sulfonated kerosene (30 vol%), and Fe^{3+} (0.36 M) as the extractant. Under optimal conditions (20 °C, O/A 1:4), they achieved 99% lithium extraction in a two-stage process. During the scrubbing stages, 6 M HCl was used to remove Al^{3+} and Mg^{2+} (O/A 40:1), and a mixture of 5.5 M LiCl with 0.5 M HCl was used to remove Ca^{2+} (O/A 30:1). Lithium stripping from organic loaded phase was performed with 6 M HCl (O/A 10:1), and the extractant was regenerated with 2 M NaOH. The following reactions were found to occur during the process:

$$Li^+{}_A + FeCl_4^-{}_A + TBP_O \rightleftarrows LiFeCl_4{\cdot}TBP_O \text{ extraction stage} \quad (28)$$

$$LiFeCl_4{\cdot}TBP_O + HCl_A \rightleftarrows LiCl_A + HFeCl_4{\cdot}TBP_O \quad \text{stripping stage} \quad (29)$$

$$HFeCl_4{\cdot}TBP_O + NaOH_A \rightleftarrows NaFeCl_4{\cdot}TBP_O + H_2O_A \quad \text{regeneration stage} \quad (30)$$

Lithium solvent extraction from coal fly ash leachate was also investigated by Cui et al. [149]. The HCl-based solution contained 0.25 g/L Li^+, 0.2 g/L Ga^{3+}, approximately 51 g/L Al^{3+}, and other cations in a total concentration of about 11 g/L. During the extraction step with TBP (O/A 1:1), high synergistic co-extraction of lithium (87%), iron (98%), and gallium (almost 100%) ions was observed due to the following reactions:

$$Li^+{}_A + FeCl_4^-{}_A + 2TBP_O \rightleftarrows [Li(TBP)_2][FeCl_4]_O \quad (31)$$

$$Li^+{}_A + GaCl_4^-{}_A + 2TBP_O \rightleftarrows [Li(TBP)_2][GaCl_4]_O \quad (32)$$

Afterward, the effective separation of metals from the loaded organic phase was achieved in consecutive steps: lithium was stripped using 6 M HCl (O/A 1:1), iron was removed with a mixture of Na_2SO_3, NaCl, and HCl (O/A 1:2), and gallium was stripped with deionized water (O/A 1:1).

TBP was further utilized as a Li^+ carrier through an ionic liquid [HOEmim][NTf_2] (i.e., 1-(2-hydroxyethyl)-3-methylimidazolium bis(trifluoromethylsulfonyl)imide) membrane, coupled with electrodialysis to drive ion migration [149]. 1 M HCl was used as a cathode solution. Selective migration of Li^+ was achieved in an acidic environment with a high concentration of aluminum ions (simulated carbon ash fly leach solution). The Al/Li ratio decreased from 30 in the feed solution to 0.55 in the receiving solution after 12 h at 3 V. Practical application in the leach liquor demonstrated that the system has preferential selectivity for transmembrane transport of Li^+, while other multivalent ions were mostly hindered.

Xu et al. [151] synthesized a resin and examined its properties for adsorbing lithium ions from strongly alkaline solutions, such as the pre-desilicated solution, a waste liquid produced during aluminum extraction from fly ash. With only 50 mg/L of Li^+ in the solution, the resin's saturated adsorption capacity reached just 0.31 mg/g. The lithium adsorption rate was positively influenced by lower temperatures, higher inlet flow rates, and higher initial lithium concentrations. The resin demonstrated good selectivity for lithium over silicon and aluminum impurities in the solution. Lithium desorption was achieved using an HCl solution.

Zhang et al. [152] developed a manganese dioxide lithium ion sieve for extracting lithium from coal fly ash leachate. The leachate was prepared by roasting desilicated coal fly ash with sodium and calcium carbonates (1200 °C, 1.5 h), followed by leaching with 5% Na_2CO_3 (150 °C, 1 h, in an autoclave). The ion sieve with the best adsorption properties was produced by mixing LiOH and MnO_2 (1:10) with water into a paste, then roasting (800 °C, 1 h), soaking in 1.5 M HCl (24 h) and stirring (18 h). This ion sieve (HMO) achieved a lithium adsorption efficiency of 99.98% under optimal conditions (0.5 h, pH 8, KOH scrubbing for 10 min). Complete lithium elution was achieved with 0.01 M HCl (40 min).

6. Lithium Recovery from Coal Bottom Ash

6.1. Coal Bottom Ash

Bottom ash, a coarse fraction of ash produced during coal combustion, typically accounts for 10%–20% of the total coal ash waste [153]. It is estimated that annual global production of coal bottom ash reaches 780 million tons, with 66% generated in Asian countries, followed by Europe and the USA [154]. Although it is mostly landfilled, posing environmental risks, its use in concrete production, as structural fills for roads, road bases, and for snow/ice control are effective methods to reduce open disposal of this waste [124,153,154].

Bottom ash consists of agglomerated particles that are too large to be carried up into the flue gases, causing them to form at the bottom of the coal furnace [111]. It is dark gray to black, granular, and highly porous (Figure 13), with particle sizes reaching up to several dozen millimeters [124].

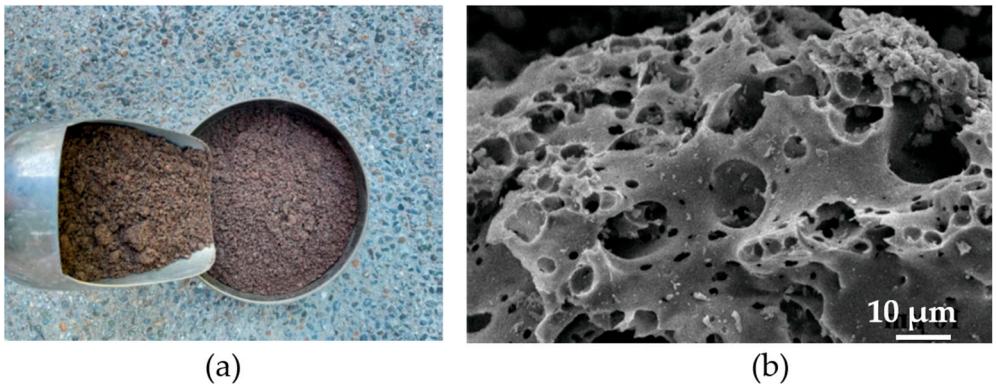


Figure 13. Coal bottom ash: (**a**) macroscopic view [155], and (**b**) SEM micrograph [156].

The main components of bottom ash are silica (39%–70%), alumina (16%–30%), and iron oxide (4%–20%), with their proportions largely dependent on the type of coal being combusted [153–158]. Bottom ash is typically more crystalline than fly ash, containing a lower proportion of the glass phase [157]. It consists of many of the same crystalline phases found in fly ash, such as quartz, mullite, magnetite, hematite, and calcite. Additionally, it can also contain unaffected sulfides, clay minerals, and carbonates [71]. While silicon, aluminum, and iron are the main components of bottom ash, elements like calcium, magnesium, sodium, and potassium are also present, along with trace amounts of Ba, B, Cr, Co, Cu, Pb, Mn, Sr, Zn, and V [71,124,159], often concentrated due to density segregation.

6.2. Occurrence Modes of Lithium

Limited literature data [71,104,131,158] provide information on lithium occurrence in bottom ashes (Table 8), but these sources indicate enrichment of lithium compared to feed coal. For instance, Karayigit et al. [71] compared lithium enrichment factors for fly and bottom ashes from a Turkish power plant, revealing a higher value for bottom ash (1.59 vs. 1.33). Similarly, Ma et al. [104] reported 143 ppm Li in bottom ash from a coal gangue power plant, which was lower than the lithium concentration in fly ash (190 ppm)

but higher than the 121 ppm Li in feed coal. Xu et al. [131] also observed lower lithium enrichment in bottom ash compared to fly ash.

Table 8. Lithium concentration in coal bottom ash.

Source	Concentration, ppm	Ref.
Republika thermoelectric power station, Bulgaria	59	[158]
Pingshuo coal gangue power plant, China	143	[104]
Chongqing power plant, China	146	[131]
Kangal power plant, Turkey	74–109	[71]

Sequential chemical extraction of lithium from bottom ash, using the procedure illustrated in Figure 8, showed that 72% of the lithium was present in the glass phase, which is nearly 20% higher than in fly ash [131]. In contrast, only about 13% of lithium was associated with mullite and quartz, which was less than half the amount found in fly ash. The distribution of lithium in other fractions (ion-exchangeable, acid-soluble, metal oxide, and organic/sulfide) was comparable between both types of ashes.

Contradictory information exists regarding the distribution of lithium across different particle fractions. Vassilev et al. [158] reported that Bulgarian bottom ash (from the combustion of sub-bituminous coal) had the lowest lithium concentration (42 ppm) in particle fractions larger than 1 mm, while the lithium concentration in smaller particle fractions remained consistent at around 61 $\pm$ 2 ppm. On the other hand, Ma et al. [104] found that in Chinese bottom ash (from the combustion of coal gangue and weathered coal), lithium concentration decreased with smaller particle sizes, a trend also observed in coal and coal gangue but opposite to that in fly ash. This effect was positively correlated with the alumina and amorphous fractions, which decreased with smaller particle diameters. Interestingly, they noted a poor correlation between lithium concentration and SiO_2 and quartz, unlike the relationship observed in feed coal.

Oboirien et al. [159] conducted laboratory studies on the impact of coal combustion conditions (900 °C or 1000 °C, combustion atmosphere) on the accumulation of lithium and other trace elements in bottom ash. They used South African coal containing approximately 50 ppm of Li. A lithium enrichment factor of 1.3 was observed in bottom ash produced from oxy-combustion (O_2/CO_2) at both temperatures, while air combustion (O_2/N_2) at 900 °C further enhanced lithium accumulation in the bottom ash.

6.3. Lithium Extraction

Although lithium enrichment in coal bottom ash is typically lower compared to fly ash, it still holds potential for utilization. However, there are currently no studies focused on optimizing the recovery conditions. Some preliminary suppositions could be drawn from leachability tests conducted to assess the impact of bottom ash on the environment. Zhang et al. [160] evaluated the leaching characteristics of alkaline coal combustion by-products. They used batch, up-flow column, and parallel bath leaching methods involving different leaching media (diluted solutions of nitric acid and potassium hydroxide, or water). Lithium can be eluted from bottom ash, but no clear trends were presented with changes in pH and solid-to-liquid ratios.

7. Conclusions

Lithium is a strategic element for many countries due to its key role in developing clean energy sources. Numerous geochemical studies cited in this work have demonstrated that lithium can be highly enriched in coal in certain regions, especially in China. Thus, these coal deposits may be a promising alternative source of lithium. Research on the modes of lithium occurrence in coal may pave the way for its possible industrial exploitation and the separation of lithium-bearing minerals (clay minerals) using mining processes.

Direct lithium leaching from coal appears inefficient, and even with thermal coal pretreatment, it seems uneconomical. Bottom ash was not assessed for lithium recovery, de-

spite being more enriched in lithium compared to feed coal. However, coal gangue and coal combustion products (mainly fly ash) represent more viable secondary lithium resources as they are less complex in composition and more enriched in lithium compared to raw coal. Lithium occurs in coal and coal by-products predominantly in inert aluminosilicate phases, necessitating a proper pretreatment stage or complex hydrometallurgical treatment to break the Si–O–Al bond of the host phase. Coal and coal gangue also require the removal of carbon to produce materials with a simpler and more homogeneous composition, reduced volume, and consequently increased lithium concentration. This enables over 90% of lithium leaching from waste materials. However, the need for material pre-treatment, the use of large amounts of leaching solutions, and relatively long leaching times during the recovery process increase the overall process costs.

Developing selective methods of lithium recovery from leachate is challenging due to the very low lithium concentrations (below 1 g/L) in the solutions, accompanied by high amounts of impurities, mainly aluminum ions. Methods for obtaining the final lithium products have not been provided, and this aspect of lithium recovery also requires clarification. Additionally, large amounts of waste liquids are likely to be generated, necessitating reuse in a closed hydrometallurgical process to avoid environmental pollution through inappropriate neutralization and discharge.

Currently, lithium extraction experiments are being conducted in laboratories, but they have only started to attract attention in recent years. The lack of pilot-scale investigations poses limitations for commercial production, which will positively be addressed in the future. Integrating lithium extraction with aluminum and silicon (and possibly other metals like rare earth elements) can represent a feasible way to reduce production costs. Advances in pretreatment, extraction, and separation processes, along with environmentally friendly waste treatment methods, will undoubtedly enhance lithium production from coal by-products for the global transition to green energy.

Funding: This research received no external funding.

Data Availability Statement: No new data were generated in this study.

Conflicts of Interest: The author declares no conflicts of interest.

References

1. Regulation (EU) 2024/1252 of the European Parliament and of the Council of 11 April 2024 Establishing a Framework for Ensuring a Secure and Sustainable Supply of Critical Raw Materials and Amending Regulations (EU) No 168/2013, (EU) 2018/858, (EU) 2018/1724 and (EU) 2019/1020 Text with EEA Relevance. Available online: https://eur-lex.europa.eu/eli/reg/2024/1252/oj (accessed on 9 July 2024).
2. Bradley, D.C.; Stillings, L.L.; Jaskula, B.W.; Munk, L.A.; McCauley, A.D. Lithium. In *Critical Mineral Resources of the United States—Economic and Environmental Geology and Prospects for Future Supply*; Schulz, K.J., De Young, J.H., Jr., Seal, R.R., II, Bradley, D.C., Eds.; U.S. Geological Survey: Reston, VA, USA, 2017; pp. K1–K21. Available online: https://pubs.usgs.gov/publication/pp1802K (accessed on 9 July 2024).
3. International Energy Agency. Global Critical Minerals Outlook 2024. 2024. Available online: https://www.iea.org/reports/global-critical-minerals-outlook-2024 (accessed on 9 July 2024).
4. Gielen, D.; Lyons, M. *Critical Materials for the Energy Transition: Lithium*; International Renewable Energy Agency: Abu Dhabi, United Arab Emirates, 2022.
5. Graham, J.D.; Rupp, J.A.; Brungard, E. Lithium in the green energy transition: The quest for both sustainability and security. *Sustainability* **2021**, *13*, 11274. [CrossRef]
6. Lindagato, P.; Li, Y.; Macháček, J.; Yang, G.; Mungwarakarama, I.; Ndahimana, A.; Ntwali, H.P.K. Lithium metal: The key to green transportation. *Appl. Sci.* **2023**, *13*, 405. [CrossRef]
7. Stampatori, D.; Raimondi, P.P.; Noussan, M. Li-ion batteries: A review of a key technology for transport decarbonization. *Energies* **2020**, *13*, 2638. [CrossRef]
8. Tsiropulos, I.; Tarvydas, D.; Lebedeva, N. *Li-Ion Batteries for Mobility and Stationary Storage Applications—Scenarios for Costs and Market Growth, EUR 29440EN*; Publications Office of the Europe Union: Luxembourg, 2018.
9. Statista. Global Lithium Industry—Statistics & Facts. Available online: https://www.statista.com/topics/3217/lithium/ (accessed on 9 July 2024).
10. Szlugaj, J.; Radwanek-Bąk, B. Lithium sources and their use. *Min. Res. Manag.* **2022**, *38*, 61–88.

11. Li, H.; Eksteen, J.; Kuang, G. Recovery of lithium from mineral resources: State-of-the-art and perspectives—A review. *Hydrometallurgy* **2019**, *189*, 105129. [CrossRef]
12. Cabello, J. Lithium brine production, reserves, resources and exploration in Chile: An updated review. *Ore Geol. Rev.* **2021**, *128*, 103883. [CrossRef]
13. Song, J.F.; Nghiem, L.D.; Li, X.M.; He, T. Lithium extraction from Chinese salt-lake brines: Opportunities, challenges, and future outlook. *Environ. Sci. Water Res. Technol.* **2017**, *3*, 593–597. [CrossRef]
14. Gao, T.M.; Fan, N.; Chen, W.; Dai, T. Lithium extraction from hard rock lithium ores (spodumene, lepidolite, zinnwaldite, petalite): Technology, resources, environment and cost. *China Geol.* **2023**, *6*, 137–153.
15. Ni, C.; Liu, C.; Wang, J.; Liang, Y.; Xie, W.; Zhong, H.; He, Z. Advances and promotion strategies of processes for extraction lithium from mineral resources. *J. Ind. Eng. Chem.* 2024, *in press*.
16. Choubey, P.K.; Kim, M.; Srivastava, R.R.; Lee, J.; Lee, J.Y. Advance review on the exploitation of the prominent energy-storage element lithium. Part I: From mineral and brine resources. *Min. Eng.* **2016**, *89*, 119–137. [CrossRef]
17. Tabelin, C.B.; Dallas, J.; Casanova, S.; Pelech, T.; Bournival, G.; Saydam, S.; Canbulat, I. Towards a low-carbon society: A review of lithium resource availability, challenges and innovations in mining, extraction and recycling, and future perspectives. *Min. Eng.* **2021**, *163*, 106743. [CrossRef]
18. Meshram, P.; Pandey, B.D.; Mankhand, T.R. Extraction of lithium from primary and secondary sources by pre-treatment, leaching and separation: A comprehensive review. *Hydrometallurgy* **2014**, *150*, 192–208. [CrossRef]
19. Kesler, S.E.; Gruber, P.W.; Medina, P.A.; Keoleian, G.A.; Everson, M.P.; Wallington, T.J. Global lithium resources: Relative importance of pegmatite, brine and other deposits. *Ore Geol. Rev.* **2012**, *48*, 55–59. [CrossRef]
20. Barbosa, H.; Soares, A.M.V.M.; Pereira, E.; Freitas, R. Lithium: A review on concentrations and impacts in marine and coastal systems. *Sci. Total Environ.* **2023**, *857*, 159374. [CrossRef]
21. Jiang, X.; Lin, X.; Yao, D.; Zhai, S.; Guo, W. Geochemistry in marine ferromanganese oxide deposits. *Deep Sea Res. I* **2007**, *54*, 85–98. [CrossRef]
22. Blutstein, K. Potential extraterrestrial sources of lithium. *Geol. Quart.* **2021**, *65*, 58.
23. Magna, T.; Wiechert, U.; Halliday, A.N. New constraints on the lithium compositions of the Moon and terrestrial planets. *Earth Plan. Sci. Lett.* **2006**, *243*, 336–353. [CrossRef]
24. Sojka, R.; Pan, Q.; Billmann, L. *Comparative Study of Li-Ion Battery Recycling Processes*; ACCUREC Recycling GmbH: Krefeld, Germany, 2020. Available online: https://accurec.de/veroeffentlichungen-downloads (accessed on 9 July 2024).
25. Knapik, E.; Rotko, G.; Marszałek, M. Recovery of lithium from oilfield brines—Current achievements and future perspectives: A mini review. *Energies* **2023**, *16*, 6628. [CrossRef]
26. Liu, Q.; Yang, P.; Tu, W.; Sun, H.; Li, S.; Zhang, Y. Lithium recovery from oil and gas produced water: Opportunities, challenges and future outlook. *J. Water Proc. Eng.* **2023**, *55*, 104148. [CrossRef]
27. Qin, S.; Zhao, C.; Li, Y.; Zhang, Y. Review of coal as a promising source of lithium. *Int. J. Oil Coal Technol.* **2015**, *9*, 215–229. [CrossRef]
28. Chen, H.; Zhang, L.; Pan, J.; Long, X.; He, X.; Zhou, C. Study on modes of occurrence and enhanced leaching of critical metals (lithium, niobum, and rare earth elements) in coal gangue. *J. Environ. Chem. Eng.* **2022**, *10*, 108818. [CrossRef]
29. Talan, D.; Huang, Q. A review study of rare Earth, cobalt, lithium, and manganese in coal-based sources and process development for their recovery. *Min. Eng.* **2022**, *189*, 107897. [CrossRef]
30. Swaine, D.J. *Trace Elements in Coal*; Butterworths: London, UK, 1990.
31. Kavanagh, L.; Keohane, J.; Cabellos, G.G.; Lloyd, A.; Cleary, J. Global lithium sources—Industrial use and future in the electric vehicle industry: A review. *Resources* **2019**, *7*, 57. [CrossRef]
32. An, J.W.; Kang, D.J.; Tran, K.T.; Kim, M.J.; Lim, T.; Tran, T. Recovery of lithium from Uyuni salar brine. *Hydrometallurgy* **2012**, *117–118*, 64–70. [CrossRef]
33. Stringfellow, W.T.; Dobson, P.F. Technology for the recovery of lithium from geothermal brines. *Energies* **2021**, *14*, 6805. [CrossRef]
34. Mends, E.A.; Chu, P. Lithium extraction from unconventional aqueous resources—A review on recent technological development for seawater and geothermal brines. *J. Environ. Chem. Eng.* **2023**, *11*, 110710. [CrossRef]
35. Choubey, P.K.; Chung, K.S.; Kim, M.; Lee, J.; Srivastava, R.R. Advance review on the exploitation of the prominent energy-storage element lithium. Part II: From sea water and spent lithium batteries (LIBs). *Min. Eng.* **2017**, *110*, 104–121. [CrossRef]
36. Artemis. Available online: https://www.nasa.gov/specials/artemis/ (accessed on 9 July 2024).
37. Liu, C.; Lin, J.; Cao, H.; Zhang, Y.; Sun, Z. Recycling of spent lithium-ion batteries in view of lithium recovery: A review. *J. Clean. Prod.* **2019**, *228*, 801–813. [CrossRef]
38. Ratuela, R.; Yadav, B.R.; Kumar, S. A review on technologies for recovery of metals from waste lithium-ion batteries. *J. Power Sourc.* **2023**, *580*, 233248. [CrossRef]
39. Cheng, Q.; Wang, Z.; Wang, Y.; Li, J.T.; Fu, H. Recent advances in preferentially selective Li recovery from spent lithium-ion batteries: A review. *J. Environ. Chem. Eng.* **2024**, *12*, 112903. [CrossRef]
40. Statista. Share of Raw Materials in Lithium-Ion Batteries, by Battery Type. Available online: https://www.statista.com/statistics/1203083/composition-of-lithium-ion-batteries/ (accessed on 9 July 2024).
41. Kumar, A.; Fukuda, H.; Hatton, T.A.; Lienhard, J.H. Lithium recovery from oil and gas produced water: A need for a growing energy industry. *ACS Energy Lett.* **2019**, *4*, 1471–1474. [CrossRef]

42. Ketris, M.P.; Yudovich, Y.E. Estimation of Clarkes for carbonaceous biolithes: World averages for trace element contents in black shales and coals. *Int. J. Coal Geol.* **2009**, *78*, 135–148. [CrossRef]
43. Sun, Y.; Li, Y.; Zhao, C.; Lin, M.; Wang, J.; Qin, S. Concentrations of lithium in Chinese coals. *Energy Explor. Exploit.* **2010**, *28*, 97–104. [CrossRef]
44. Liu, C.; Zhao, T.; Wang, G.; Chen, D. A review of China's resources of lithium in coal seams. *Front. Energy Res.* **2024**, *12*, 1008320. [CrossRef]
45. Dai, S.F.; Ren, D.Y.; Chou, C.L.; Li, S.S.; Jiang, Y.F. Mineralogy and geochemistry of the No. 6 Coal (Pennsylvanian) in the Junger Coalfield, Ordos Basin, China. *Int. J. Coal Geol.* **2006**, *66*, 253–270. [CrossRef]
46. Dai, S.F.; Li, D.; Chou, C.L.; Zhao, L.; Zhang, Y.; Ren, D.Y.; Ma, Y.; Sun, Y. Mineralogy and geochemistry of boehmite-rich coals: New insights from the Haerwusu Surface Mine, Jungar Coalfield, Inner Mongolia, China. *Int. J. Coal Geol.* **2008**, *74*, 185–202. [CrossRef]
47. Sun, Y.; Zhao, C.; Zhang, J.; Yang, J.; Zhang, Y.; Yuan, Y.; Xu, J.; Duan, D. Concentrations of valuable elements of the coals from the Pingshuo Mining District, Ningwu Coalfield, northern China. *Energy Explor. Exploit.* **2013**, *31*, 727–744. [CrossRef]
48. Sun, Y.Z.; Zhao, C.L.; Li, Y.H.; Wang, J.X.; Lin, M.Y. Li distribution and mode of occurrences in Li-bearing coal seam 9 from Pingshuo Mining District, Ningwu Coalfield, northern China. *Energy Educ. Sci. Technol. Part A Energy Sci. Res.* **2013**, *31*, 27–38.
49. Zhao, L.; Dai, S.; Nechaev, V.P.; Nechaeva, E.V.; Graham, I.T.; French, D. Enrichment origin of critical elements (Li and rare earth elements) and a Mo-U-Se-Re assemblage in Pennsylvanian anthracite from the Jincheng Coalfield, southeastern Qinshui Basin, northern China. *Ore Geol. Rev.* **2019**, *115*, 103184. [CrossRef]
50. Seredin, V.V.; Dai, S.; Sun, Y.; Chekryzhov, I.Y. Coal deposits as promising source of rare metals for alternative power and energy-efficient technologies. *Appl. Geochem.* **2013**, *31*, 1–11. [CrossRef]
51. Wang, Q.; Yan, Q.; Zhang, Y.; Zhou, F. Enrichment mechanism of lithium in late Permian coals in the Bijie Area, Guizhou, China. *ACS Omega* **2022**, *7*, 16361–16370. [CrossRef]
52. Lin, R.; Soong, Y.; Granite, E.J. Evaluation of trace elements in U.S. coals using the USGS COALQUAL database version 3.0. Part II: Non-REY critical elements. *Int. J. Coal Geol.* **2018**, *192*, 39–50. [CrossRef]
53. Dale, L.; Lavrencic, S. Trace elements in Australian export thermal coals. *Austral. Coal J.* **1993**, *39*, 17–21.
54. Pougnet, M.A.B.; Wyrleybirch, J.M.; Orren, M.J. The boron and lithium content of South-African coals and coal ashes. *Int. J. Environ. Anal. Chem.* **1990**, *38*, 539–549. [CrossRef]
55. Arbuzov, S.I.; Chekruzhov, I.Y.; Spears, D.A.; Ilenok, S.S.; Soktoev, B.R.; Popov, N.Y. Geology, geochemistry, mineralogy and genesis of the Spetsugli high–germanium coal deposit in the Pavlovsk coalfield, Russian Far East. *Ore Geol. Rev.* **2021**, *139*, 104537. [CrossRef]
56. Palmer, C.A.; Tuncali, E.; Dennen, K.O.; Coburn, T.C.; Finkelman, R.B. Characterization of Turkish coals: A nationwide perspective. *Int. J. Coal. Geol.* **2004**, *60*, 85–115. [CrossRef]
57. Finkelman, R.B.; Palmer, C.A.; Wang, P. Quantification of the modes of occurrence of 42 elements in coal. *Int. J. Coal Geol.* **2018**, *185*, 138–160. [CrossRef]
58. Zhang, W.; Noble, A.; Yang, X.; Honaker, R. Lithium leaching recovery and mechanisms from density fractions of an Illinois Basin bituminous coal. *Fuel* **2020**, *268*, 117319. [CrossRef]
59. Zhang, W.; Honaker, R. Characterization and recovery of rare earth elements and other critical metals (Co, Cr, Li, Mn, Sr, and V) from the calcination products of a coal refuse sample. *Fuel* **2020**, *267*, 117236. [CrossRef]
60. Das, A.; Kumar, R.; Patel, S.S.; Saha, C.; Das, A.; Mandal, H.; Patel, R.S. Geochemical variations of major, trace, rare earth elements in some Gondwana and Eocene coals of India with a comparison of their germanium, lithium, and mercury content. *Geochemistry* **2023**, *83*, 125960. [CrossRef]
61. Statista. Distribution of Coal Production Worldwide in 2023, by Major Countries. Available online: https://www.statista.com/statistics/265638/distribution-of-coal-production-worldwide/ (accessed on 9 June 2024).
62. Zou, J.; Cheng, L.; Guo, Y.; Wang, Z.; Tian, H.; Li, T. Mineralogical and geochemical characteristics of lithium and rare earth elements in high-sulfur coal from the Donggou Mine, Chongqing, Southwestern China. *Minerals* **2020**, *10*, 627. [CrossRef]
63. Sun, Y.; Yang, J.; Zhao, C. Minimum mining grade of associated Li deposits in coal seams. *Energy Explor. Exploit.* **2012**, *30*, 167–170. [CrossRef]
64. Wang, G.; Xie, Y.; Qin, Y.; Wang, J.; Shen, J.; Han, B.; Liang, C.; Wang, Q. Element geochemical characteristics and formation environment for the roof, floor and gangue of coal seems in the Guijao mining area, Xishan coalfield, China. *J. Geochem. Explor.* **2018**, *190*, 336–344. [CrossRef]
65. Qin, G.; Cao, D.; Wei, Y.; Wang, A.; Liu, J. Mineralogy and geochemistry of the No.5^{-2} high–sulfur coal from the Dongpo Mine, Weibei Coalfield, Shaanxi, north China, with emphasis on anomalies of gallium and lithium. *Minerals* **2019**, *9*, 402. [CrossRef]
66. Li, X.; Wei, Y.; Cao, D.; Wei, J.; Liu, X.; Zhang, Y.; Dong, B. Cooperative exploration model of coal-lithium deposit: A case study of the Haerwusu coal-lithium deposit in the Jungar Coalfild, Inner Mongolia, Northern China. *Minerals* **2024**, *14*, 179. [CrossRef]
67. Dai, S.; Wang, X.; Zhou, Y.; Hower, J.C.; Li, D.; Chen, W.; Zhu, X.; Zou, J. Chemical and mineralogical compositions of silicic, mafic, and alkali tonsteins in the late Permian coals from the Songzao Coalfield, Chongqing, Southwest China. *Chem. Geol.* **2011**, *282*, 29–44. [CrossRef]
68. Coal Production. Energy Institute—Statistical Review of World Energy (2024). The Shift Data Portal (2019). Available online: https://ourworldindata.org/grapher/coal-production-by-country (accessed on 19 June 2024).

69. Arbuzov, S.I.; Chekryzhov, I.Y.; Verkhoturov, A.A.; Spears, D.A.; Melkiy, V.A.; Zarubina, N.V.; Blokhin, M.G. Geochemistry and rare-metal potential of coals of the Sakhalin coal basin, Sakhalin island, Russia. *Int. J. Coal Geol.* **2023**, *268*, 104197. [CrossRef]
70. Lehmden, D.J.; Jungers, R.H.; Lee, R.E. Determination of trace elements in coal, fly ash, fuel oil, and gasoline—A preliminary comparison of selected analytical techniques. *Anal. Chem.* **1974**, *46*, 239–245. [CrossRef]
71. Karayigit, A.I.; Oskay, R.G.; Gayer, R.A. Mineralogy and geochemistry of the Kangal power plant (Sivas, Turkey). *Turk. J. Earth Sci.* **2019**, *28*, 438–456. [CrossRef]
72. Querol, X.; Fernandez-Turiel, L.J.; Lopez-Soler, A. Trace elements in coal and their behaviour during combustion in a large power station. *Fuel* **1995**, *74*, 311–343. [CrossRef]
73. Balaram, V.; Santosh, M.; Satyanarayanan, M.; Srinivas, N.; Gupta, H. Lithium: A review of applications, occurrence, exploration, extraction, recycling, analysis, and environmental impact. *Geosci. Front.* **2024**, *15*, 101868. [CrossRef]
74. Lewińska-Preis, L.; Fabiańska, M.J.; Ćmiel, S.; Kita, A. Geochemical distribution of trace elements in Kaffioyra and Longyearbyen coals, Spitsbergen, Norway. *Int. J. Coal Geol.* **2009**, *80*, 211–223. [CrossRef]
75. Dai, S.; Finkelman, R.B.; French, D.; Hower, J.C.; Graham, I.T. Modes of occurrence of elements in coal: A critical evaluation. *Earth Sci. Rev.* **2021**, *222*, 103815. [CrossRef]
76. Wang, X.; Wang, X.; Pan, Z.; Pan, W.; Yin, X.; Chai, P.; Pan, S.; Yang, Q. Mineral and geochemical characteristics of the Permian coal from the Qinshui basin, northern China, with emphasis on lithium enrichment. *Int. J. Coal Geol.* **2019**, *217*, 103254. [CrossRef]
77. Vejahati, F.; Xu, Z.; Gupta, R. Trace elements in coal: Associations with coal and minerals and their behavior during coal utilization—A review. *Fuel* **2010**, *89*, 904–911. [CrossRef]
78. Yossifova, M.G. Mineral and inorganic chemical composition of the Pernik coal, Bulgaria. *Int. J. Coal. Geol.* **2007**, *72*, 268–292. [CrossRef]
79. Zhang, W.; Zhao, L.; Wang, W.; Neachaev, V.P.; French, D.; Graham, I.; Lang, Y.; Li, Z.; Dai, S. Enrichment of critical metals (Li, Ga, and rare earth elements) in the early Permian coal seam from the Jincheng Coalfield, southeastern Qinshui Basin, northern China: With an emphasis on cookeite as the li host. *Ore Geol. Rev.* **2024**, *167*, 105939. [CrossRef]
80. Fossil Fuels. Energy Institute—Statistical Review of World Energy (2024). The Shift Data Portal (2019). Available online: https://ourworldindata.org/fossil-fuels (accessed on 19 June 2024).
81. Li, J.; Wang, J. Comprehensive utilization and environmental risk of coal gangue: A review. *J. Clean. Prod.* **2019**, *239*, 117946. [CrossRef]
82. Haibin, L.; Zhenling, L. Recycling utilization patterns of coal mining waste in China. *Res. Cons. Rec.* **2010**, *54*, 1331–1340. [CrossRef]
83. Song, W.; Zhang, J.; Li, M.; Yan, H.; Zhou, N.; Yao, Y.; Guo, Y. Underground disposal of coal gangue backfill in China. *Appl. Sci.* **2022**, *12*, 12060. [CrossRef]
84. Yaofei, L.; Xingchen, Z.; Ke, Z. Coal gangue in asphalt pavement: A review of applications and performance influence. *Case Stud. Constr. Mater.* **2024**, *20*, e03282. [CrossRef]
85. Tan, W.F.; Wang, L.A.; Huang, C. Environmental effects of coal gangue and its utilization. *Energy Sources Part A Recovery Util. Environ. Eff.* **2016**, *38*, 3716–3721. [CrossRef]
86. Duan, D.; Wang, C.; Bai, D.; Huang, D. Representative coal gangue in China: Physical and chemical properties, heavy metal coupling mechanism and risk assessment. *Sustain. Chem. Pharm.* **2024**, *37*, 101402. [CrossRef]
87. Hu, F.; Zhou, M.; Dai, R.; Liu, Y. Recognition method of coal and gangue based on multispectral characteristics combined with one-dimensional convolutional neural network. *Front. Earth Sci.* **2022**, *10*, 893485. [CrossRef]
88. Zheng, Q.; Zhou, Y.; Liu, X.; Liu, M.; Liao, L.; Lv, G. Environmental hazards and comprehensive utilization of solid waste coal gangue. *Prog. Nat. Sci. Mater. Int.* **2024**, *34*, 223–239. [CrossRef]
89. Dong, J.; Li, J.; Huang, Y.; Zhong, J.; Dun, K.; Wu, M.; Zhang, L.; Chen, Q.; Pan, B. Understanding the release, migration, and risk of heavy metals in coal gangue: An approach by combining experimental and computational investigations. *J. Hazard. Mater.* **2024**, *461*, 132707. [CrossRef]
90. Gao, H.; Huang, Y.; Li, W.; Li, J.; Ouyang, S.; Song, T.; Lv, F.; Zhai, W.; Ma, K. Explanation of heavy metal pollution in coal mines of China from the perspective of coal gangue geochemical characteristics. *Environ. Sci. Poll. Res.* **2021**, *28*, 65363–65373. [CrossRef]
91. Zhang, L.; Chen, H.; Pan, J.; Wen, Z.; Shi, S.; Long, X.; Zhou, C. The effect of physical separation and calcination on enrichment and recovery of critical elements from coal gangue. *Minerals* **2022**, *12*, 1371. [CrossRef]
92. Li, J.; Liu, L.; Kang, X.; Li, K.; Zhang, S.; Liu, Q. Enrichment of lithium in the claystone coal gangue from the Malan mine, Xishan Coalfield, Shanxi Province, Northern China. *Geochemistry* **2023**, *83*, 125972.
93. Dai, S.; Sun, F.; Wang, L.; Wang, L.; Zhang, R.; Guo, H.; Xing, Y.; Gui, X. A new method for pre-enrichment of gallium and lithium based on mode of occurrence in coal gangue from Antaibao surface mine, Shanxi Province, China. *J. Clean. Prod.* **2023**, *425*, 138968. [CrossRef]
94. Shao, S.; Ma, B.; Wang, C.; Chen, Y. Extraction of valuable components from coal gangue through thermal activation and HNO_3 leaching. *J. Ind. Eng. Chem.* **2022**, *113*, 564–574. [CrossRef]
95. Qin, Q.; Deng, J.; Geng, H.; Bai, Z.; Gui, X.; Ma, Z.; Miao, Z. An exploratory study on strategic metal recovery of coal gangue and sustainable utilization potential of recovery residue. *J. Clean. Prod.* **2022**, *340*, 130765. [CrossRef]
96. Qin, Q.; Geng, H.; Deng, J.; Su, X.; Chen, M.; Park, C.B. Al and other critical metals co-extraction from coal gangue through delamination pretreatment and recycling strategies. *Chem. Eng. J.* **2023**, *477*, 147036. [CrossRef]

97. Zhang, L.; Chen, H.; Pan, J.; Yang, F.; Liu, H.; Zhou, C.; Zhang, N. Extraction of lithium from coal gangue by roasting-leaching process. *Int. J. Coal Prep. Util.* **2023**, *43*, 863–878. [CrossRef]
98. Xie, Y.; Ni, C.; Wu, M.; Han, Z.; Liao, J.; Nie, S.; He, Z.; Xie, W. Recycling strategy toward efficient and green lithium leaching from coal-based lithium ores enabled by solubility engineering and reusable solid acid. *ACS Sustain. Chem. Eng.* **2023**, *11*, 2910–2916. [CrossRef]
99. Xie, Y.; Ni, C.; Han, Z.; Liao, J.; Xie, W.; Zhong, H.; He, Z. Recovery of lithium from coal gangue utilizing acid baking followed by water leaching. *Int. J. Coal Prep. Util.* **2024**, *44*, 82–94. [CrossRef]
100. Kang, C.; Yang, S.; Qiao, J.; Zhao, Y.; Dong, S.; Wang, Y.; Duan, C.; Liu, J. Extraction of valuable critical metals from coal gangue by roasting activation-sulfuric acid leaching. *Int. J. Coal Prep. Util.* 2024, *in press*. [CrossRef]
101. Chen, H.; Zhang, L.; Pan, J.; He, X.; Shi, S.; Long, X.; Yang, Y.; Zhao, X.; Zhou, C. Study on modes of occurrence and selective leaching of lithium in coal gangue via grinding-thermal activation. *Chem. Eng. J.* **2024**, *482*, 148941. [CrossRef]
102. Xie, Y.; Ni, C.; Han, Z.; Zhong, H.; He, Z.; Sun, W. High recovery of lithium from coal residue by roasting and sulfuric acid leaching. *Min. Eng.* **2023**, *202*, 108284. [CrossRef]
103. Fang, D.; Xia, Y.; Li, Y.; Xing, Y.; Miao, Z.; Gui, X. Separation and recovery of valuable carbon components and Li/Ga metals in coal gangue by using a flotation flowsheet. *ACS Omega* **2024**, *9*, 14336–14342. [CrossRef]
104. Ma, Z.; Shan, X.; Cheng, F. Distribution characteristics of valuable elements, Al, Li, and Ga, and rare earth elements in feed coal, fly ash, and bottom ash from 300 MW circulating fluidized bed boiler. *ACS Omega* **2019**, *4*, 6854–6863. [CrossRef] [PubMed]
105. Tessier, A.; Campbell, P.G.C.; Bisson, M. Sequential extraction procedure for the speciation of particulate trace metals. *Anal. Chem.* **1979**, *51*, 844–851. [CrossRef]
106. Davidson, C.M.; Thomas, R.P.; McVey, S.E.; Perala, R.; Littlejohn, D.; Ure, A.M. Evaluation of a sequential extraction procedure for the speciation of heavy metals in sediments. *Anal. Chim. Acta.* **1994**, *291*, 277–286. [CrossRef]
107. Swain, B. Recovery and recycling of lithium: A review. *Sep. Purif. Technol.* **2017**, *172*, 388–403. [CrossRef]
108. Butylskii, D.Y.; Troitskiy, V.A.; Smirnova, N.V.; Pismenskaya, N.D.; Wang, Y.; Jiang, C.; Xu, T.; Nikonenko, V.V. Review of recent progress on lithium recovery and recycling from primary and secondary sources with membrane-based technologies. *Desalination* **2024**, *586*, 117826. [CrossRef]
109. Mojid, M.R.; Lee, K.J.; You, J. A review on advances in direct lithium extraction from continental brines: Ion-sieve adsorption and electrochemical methods for varied Mg/Li ratios. *Sustain. Mater. Technol.* **2024**, *40*, e00923. [CrossRef]
110. Long, X.; Liu, C.; Yang, Y.; Dong, B.; Chen, H.; Zhang, L.; Pan, J.; Zhou, C. Microwave-assisted hydrothermal synthesis of lithium ion-sieve for adsorption of lithium ion in coal gangue leaching solution. *Colloids Surf. A Physicochem. Eng. Asp.* **2024**, *682*, 132819. [CrossRef]
111. EPA United States Environmental Protection Agency. Coal Ash (Coal Combustion Residuals). Available online: https://www.epa.gov/coalash (accessed on 19 June 2024).
112. Zierold, C.; Odoh, C. A review on fly ash from coal-fired power plants: Chemical composition, regulations, and health evidence. *Rev. Environ. Health* **2020**, *35*, 401–418. [CrossRef]
113. Nsiah-gyambibi, R.; Sokama-Neuyam, Y.A.; Bokakye, P.; Ampomah, W.; Aggrey, W.N.; Wang, S. Valorization of coal fly ash (CFA): A multi-industry review. *Int. J. Environ. Sci. Technol.* **2023**, *20*, 12807–12822. [CrossRef]
114. Baig, S.Y.; Yousaf, M. Coal fired power plants: Emission problems and controlling techniques. *J. Earth Sci. Clim. Chang.* **2017**, *8*, 104. [CrossRef]
115. Wang, N.; Sun, X.; Zhao, Q.; Yang, Y.; Wang, P. Leachability and adverse effects of coal fly ash: A review. *J. Hazard. Mater.* **2020**, *396*, 122725. [CrossRef] [PubMed]
116. Das, D.; Rout, P.K. A review of coal fly as utilization to save the environment. *Water Air Soil Pollut.* **2023**, *234*, 128. [CrossRef]
117. Yao, Z.T.; Ji, X.S.; Sarker, P.K.; Tang, J.H.; Ge, L.Q.; Xia, M.S.; Xi, Y.Q. A comprehensive review in the applications of coal fly ash. *Earth Sci. Rev.* **2015**, *141*, 105–121. [CrossRef]
118. Vilakazi, A.Q.; Ndlovu, S.; Chisie, L.; Shemi, A. The recycling of coal fly ash: A review on sustainable developments and economic considerations. *Sustainability* **2022**, *14*, 1958. [CrossRef]
119. Gollakota, A.R.K.; Volli, V.; Shu, C.M. Progressive utilization prospects of coal fly ash: A review. *Sci. Total Environ.* **2019**, *672*, 951–989. [CrossRef]
120. Putilova, I.V. Current state of the coal ash handling problem in Russia and abroad, aspects of the coal ash applications in hydrogen economy. *Int. J. Hydrog. Energy* **2023**, *48*, 31040–31048. [CrossRef]
121. Zhao, S.; Duan, Y.; Lu, J.; Gupta, R.; Pudasainee, D.; Liu, S.; Liu, M.; Lu, J. Chemical speciation and leaching characteristics of hazardous trace elements in coal and fly ash from coal-fired power plants. *Fuel* **2018**, *232*, 463–469. [CrossRef]
122. Strzałkowska, E. Fly ash—A valuable material for the circular economy. *Min. Res. Manag.* **2021**, *37*, 49–62.
123. Cui, H.; Sheng, X.; Hu, S.; Li, S.; Zhang, S.; Zhou, J. Impacts of modified fly ash on soil available lead and copper and their accumulation by ryegrass. *Agronomy* **2023**, *13*, 2194. [CrossRef]
124. Meawad, A.S.; Bojinova, D.Y.; Pelovski, Y.G. An overview of metals recovery from thermal power plant solid wastes. *Waste Manag.* **2010**, *30*, 2548–2559. [CrossRef]
125. Vig, N.; Mor, S.; Ravindra, K. The multiple value characteristics of fly ash from Indian coal thermal power plants: A review. *Environ. Monit. Assess.* **2023**, *195*, 33. [CrossRef] [PubMed]

126. Medina, A.; Gamero, P.; Querol, X.; Moreno, N.; De Leon, B.; Almanza, M.; Vargas, G.; Izquierdo, M.; Font, O. Fly ash from a Mexican mineral coal: Mineralogical and chemical characterization. *J. Hazard. Mater.* **2010**, *181*, 72–90. [CrossRef] [PubMed]
127. Moreno, N.; Querol, X.; Andres, J.M.; Stanton, K.; Towler, M.; Nugteren, H.; Janssen-Jurkovicova, M.; Jones, R. Physico-chemical characteristic of European pulverized coal combustion fly ashes. *Fuel* **2005**, *84*, 1351–1363. [CrossRef]
128. Pentari, D.; Vlachaki, E.; Fazaki, M.E.; Stratakis, A. Lithium in Greek coal fly ashes: Contents and characterization by sequential extraction. *Sustainability* **2024**, *16*, 1442. [CrossRef]
129. Hu, P.; Hou, X.; Zhang, J.; Li, S.; Wu, H.; Damo, A.J.; Li, H.; Wu, Q.; Xi, X. Distribution, and occurrence of lithium in high-alumina coal fly ash. *Int. J. Coal Geol.* **2018**, *189*, 27–34. [CrossRef]
130. Dai, S.; Zhao, L.; Peng, S.; Chou, C.L.; Wang, X.; Zhang, Y.; Li, D.; Sun, Y. Abundances and distribution of minerals and elements in high-alumina coal fly ash from the Jungar Power Plant, Inner Mongolia, China. *Int. J. Coal Geol.* **2010**, *81*, 320–332. [CrossRef]
131. Xu, F.; Qin, S.; Li, S.; Wang, J.; Qi, D.; Lu, Q.; Xing, J. Distribution, occurrence mode, and extraction potential of critical elements in coal ashes of the Chongqing Power Plant. *J. Clean. Prod.* **2022**, *342*, 130910. [CrossRef]
132. Shao, P.; Hou, H.; Wang, W.; Wang, W. Geochemistry and mineralogy of fly ash from the high-alumina coal, Datong Coalfield, Shanxi, China. *Ore Geol. Rev.* **2023**, *158*, 105476. [CrossRef]
133. Xu, F.; Qin, S.; Li, S.; Wen, H.; Lv, H.; Wang, Q.; Kang, S. The migration and mineral host changes of lithium during coal combustion: Experimental and thermodynamic calculation study. *Int. J. Coal Geol.* **2023**, *275*, 104298. [CrossRef]
134. Li, C.; Zhou, C.; Li, W.; Zhu, W.; Shi, J.; Liu, G. Enrichment of critical elements from coal fly ash by the combination of physical separations. *Fuel* **2023**, *336*, 127156. [CrossRef]
135. Li, S.; Qin, S.; Kang, L.; Liu, J.; Wang, J.; Li, Y. An efficient approach for lithium and aluminum recovery from coal fly ash by pre-silication and intensified acid leaching processes. *Metals* **2017**, *7*, 272. [CrossRef]
136. Xu, H.; Liu, C.; Mi, X.; Wang, Z.; Han, J.; Zeng, G.; Liu, P.; Guan, Q.; Ji, H.; Huang, S. Extraction of lithium from coal fly ash by low-temperature ammonium fluoride activation-assisted leaching. *Sep. Purif. Technol.* **2021**, *279*, 119757. [CrossRef]
137. Rezaei, H.; Shafaei, S.Z.; Abdollahi, H.; Shahidi, A.; Ghassa, S. A sustainable method for germanium, vanadium and lithium extraction from coal fly ash: Sodium salts roasting and organic acids leaching. *Fuel* **2022**, *312*, 122844. [CrossRef]
138. Rezaei, H.; Shafaei, S.Z.; Abdollahi, H.; Ghassa, S.; Boroumand, Z.; Nosratabad, A.F. Spent-medium leaching of germanium, vanadium and lithium from coal fly ash with biogenic carboxylic acids and comparison with chemical leaching. *Hydrometallurgy* **2023**, *217*, 106038. [CrossRef]
139. Xing, M.; Zhang, F.; Zheng, P.; Wang, Y.; Zhao, L.; Xu, C. Selective recovery of lithium from high-aluminum fly ash by using alkali dissolution-assisted HBTA-TPO synergistic extraction. *J. Clean. Prod.* **2024**, *434*, 139998. [CrossRef]
140. Fang, H.; Zhou, C.; Xu, S.; Shi, J.; Hu, Y.; Liu, G. High-efficiency extraction of aluminum and lithium from coal fly ash using a novel sodium pyrosulfate mechanochemical activation—Sodium persulfate pressure leaching technology. *J. Clean. Prod.* **2023**, *423*, 138841. [CrossRef]
141. Li, C.; Zhou, C.; Li, W.; Zhu, W.; Shi, J.; Wu, L.; Liu, G. A two-stage process of alkali fusion and organic acid leaching for recovery of critical elements from coal fly ash. *J. Ind. Eng. Chem.* **2024**, *138*, 131–143. [CrossRef]
142. Gao, R.; Peng, H.; He, Q.; Meng, Z.; Xiang, P.; Hou, L.; Miao, Z. Simultaneous leaching of Li, Ga, and REE from coal fly ash and novel method for selective leaching of Li and Ga. *J. Environ. Chem. Eng.* **2024**, *12*, 112022. [CrossRef]
143. Ma, Z.; Zhang, S.; Zhang, H.; Cheng, F. Novel extraction of valuable metals from circulating fluidized bed-derived high alumina fly ash by acid-alkali based alternate method. *J. Clean. Prod.* **2019**, *230*, 302–313. [CrossRef]
144. Li, J.; Gao, J.M.; Guo, Y.; Cheng, F. Energy-efficient leaching process for preparation of aluminum sulfate and synergistic extraction of Li and Ga from circulating fluidized bed fly ash. *Energy Sources Part A Recovery Util. Environ. Eff.* **2022**, *44*, 4398–4410. [CrossRef]
145. Sahoo, K.; Kim, K.; Powell, M.A.; Equeenuddin, S.M. Recovery of metals and other beneficial products from coal fly ash: A sustainable approach for fly ash management. *Int. J. Coal Technol.* **2016**, *3*, 267–283. [CrossRef]
146. Gong, Y.; Sun, J.; Zhang, Y.; Zhang, Y.; Zhang, T. Dependence on the distribution of valuable elements and chemical characterizations based on different particle sizes of high alumina fly ash. *Fuel* **2021**, *191*, 120225. [CrossRef]
147. Chen, M.; Gong, Y.; Zhang, X.; Zhao, X.; Chen, T.; Batdelger, B.; Bold, T. Comprehensive analysis of thermochemical phase evolution and strategic recovery of valuable elements from high-alumina coal fly ash at different thermal conditions. *Fuel* **2024**, *367*, 131490. [CrossRef]
148. Rui, H.; Zhang, L.; Li, L.; Zhu, L. Solvent extraction of lithium from hydrochloric acid leaching solution of high alumina coal fly ash. *Chem. Phys. Lett.* **2021**, *771*, 138510. [CrossRef]
149. Cui, L.; Feng, L.; Yuan, H.; Cheng, H.; Cheng, F. Efficient recovery of aluminum, lithium, iron and gallium from coal fly ash leachate via coextraction and stepwise stripping. *Res. Cons. Rec.* **2024**, *202*, 107380. [CrossRef]
150. Cui, L.; Zhang, Q.; Li, C.; Wang, L.; Sun, D.; Cheng, F. Liquid membrane coupled electrodialysis system for highly-efficient lithium recovery from fly ash acid leaching solution. *Chem. Eng. Process. Proc. Inten.* **2024**, *195*, 109650. [CrossRef]
151. Xu, Z.; Wang, X.; Sun, S. Performance of a synthetic resin for lithium adsorption in waste liquid of extracting aluminum from fly-ash. *Chin. J. Chem. Eng.* **2022**, *44*, 115–123. [CrossRef]
152. Zhang, P.; Li, Y.; Xu, M.; Yao, B.; Zhang, C. Preparation of manganese dioxide lithium sieve and its application in lithium extraction from coal fly ash. *Appl. Sci.* **2024**, *14*, 1463. [CrossRef]

153. Mohammed, S.A.; Koting, S.; Katman, H.Y.B.; Babalghaith, A.M.; Patah, M.F.A.; Ibrahim, M.R.; Karim, M.R. A review of the utilization of coal bottom ash (CBA) in the construction industry. *Sustainability* **2021**, *13*, 8031. [CrossRef]
154. Tamanna, K.; Raman, S.N.; Jamil, M.; Hamid, R. Coal bottom ash as supplementary material for sustainable construction: A comprehensive review. *Constr. Build. Mater.* **2023**, *389*, 131679. [CrossRef]
155. Seav, N.; Kim, K.S.; Kim, J.H.; Lee, S.W.; Kim, Y.K. Effects of roller compacted concrete incorporating coal bottom ash as a fine aggregate replacement. *Sustainability* **2023**, *15*, 11420. [CrossRef]
156. Abbas, S.; Arshad, U.; Abbas, W.; Nehdi, M.L.; Ahmed, A. Recycling untreated coal bottom ash with added value for mitigating alkali-silica reaction in concrete: A sustainable approach. *Sustainability* **2020**, *12*, 10631. [CrossRef]
157. Zheng, Y.; Zhao, L.; French, D.; Graham, I.; Wei, Q.; Dai, S.; Feng, L. Revisiting sustainable resources in the combustion products of alumina-rich coal: Critical metal (Li, Ga, Nb, and REY) potential of ash from the Togtoh Power Plant, Inner Mongolia, China. *Sci. Total Environ.* **2024**, *950*, 175056. [CrossRef]
158. Vassilev, S.V.; Eskenazy, G.M.; Vassileva, C.G. Behaviour of elements and minerals during preparation and combustion of the Pernik coal, Bulgaria. *Fuel Proc. Technol.* **2001**, *72*, 103–109. [CrossRef]
159. Oboirien, B.O.; Thulari, V.; North, B.C. Major and trace elements in coal bottom ash at different oxy coal combustion conditions. *Appl. Energy* **2014**, *129*, 207–216. [CrossRef]
160. Zhang, S.; Dai, S.; Finkelman, R.B.; Graham, I.T.; French, D.; Hower, J.C.; Li, X. Leaching characteristics of alkaline coal combustion by-products: A case study from a coal-fired power plant, Hebei Province, China. *Fuel* **2019**, *255*, 115710. [CrossRef]

Disclaimer/Publisher's Note: The statements, opinions and data contained in all publications are solely those of the individual author(s) and contributor(s) and not of MDPI and/or the editor(s). MDPI and/or the editor(s) disclaim responsibility for any injury to people or property resulting from any ideas, methods, instructions or products referred to in the content.